Low Temperature Physics/Fizika Nizkikh Temperatur, 2013, v. 39, No. 3, pp. 301–319

Charge density waves in *d*-wave superconductors: thermodynamics and Josephson tunneling

(Review Article)

A.M. Gabovich and A.I. Voitenko

Institute of Physics, National Academy of Sciences of Ukraine
46 Nauka Ave., Kyiv 03028, Ukraine
E-mail: gabovich@iop.kiev.ua

Received October 25, 2012

The problem of coexistence between charge-density-waves (CDWs) and superconductivity is revisited. Recent evidence was analyzed for different classes of materials with the emphasis on high-T_c oxides. For the latter, the model of the *d*-wave or extended *s*-wave Cooper pairing competing with checkerboard or unidirectional CDWs is suggested. The corresponding phase diagrams were plotted and used as a guide to predict new features in the tunnel or photoemission spectra. In the framework of the model concerned, dc Josephson tunneling through junctions involving CDW superconductors is examined. It is shown that CDWs distort current dependences on the angle between crystal axes and the junction plane inherent to *d*-wave superconductors leading to an extra periodicity.

PACS: 74.20.Fg BCS theory and its development;
74.20.Rp Pairing symmetries (other than *s*-wave);
74.50.+r Tunneling phenomena; Josephson effects;
74.72.–h Cuprate superconductors;
71.45.Lr Charge-density-wave systems.

Keywords: charge-density-wave superconductors, *d*-pairing, cuprates, phase diagram, dc Josephson effect.

Contents

1. Introduction

We are happy to present our article in this issue devoted to the memory of a great scientist Igor Kondratievich Yanson, who was one of the world leaders in the Josephson-effect physics [1,2] and made a seminal contribution to the condensed matter science as a whole. In particular, he developed a new method of point-contact spectroscopy and systematically applied it to study conventional and exotic materials [3–8]. This spectroscopic method and its "elder

sister", tunneling spectroscopy [8,9–17], invoked a substantial progress in investigations of materials discussed in this review.

Condensed matter science being the basis of the modern industry needs a variety of materials for diverse applications [18]. Some solids reveal long-range orderings of various kinds [19] which develop against a crystal-lattice background in certain temperature, T, ranges. In this connection, one can mention magnetic states (ferromagnetism, antiferromagnetism, spin density waves — SDWs) [20,21], ferro- and antiferro-electricity [22], charge density waves — CDWs (with concomitant periodic lattice distortions, PLDs) [8,19, 21,23], and superconductivity [24,25]. These states can coexist under favorable conditions inducing mixed phases, e.g., multiferroics [26] and CDW or SDW superconductors [8,27–33]. The properties of mixed phases are interesting *per se* and deserve a thorough investigation. Moreover, in the case of CDW superconductors, the interplay between constituents is important because the combined structural and electron-spectrum instabilities compete with Cooper pairing and might be the main factor limiting the magnitude of the critical temperature, T_c [34–36]. The opposite viewpoint that the high density of states near the edges of the dielectric (CDW or SDW) gap promotes superconductivity [37–39] in the spirit of the original Bardeen-Cooper-Schrieffer (BCS) model [40] has not been confirmed by even a single experiment and, hence, it is not discussed below.

As for high-T_c cuprates, we consider pseudogaps observed there with the help of different methods [41–48] as manifestations of CDWs in the mixed "CDW + superconductor" state (see the relevant argumentation below and in our previous publications [27–31]). Therefore, the terms "pseudogaps" and "CDW gaps" for cuprates are assumed identical throughout the paper.

Within the period since our last reviews [30,31] on the topic of coexistence between CDWs and superconductivity have been published, more experimental and theoretical studies concerning CDW superconductors have been carried out. In this Review, information about these materials is updated and our original theory of the coexisting CDWs and unconventional (*d*-wave and extended *s*-wave) superconductivity is outlined, with the special emphasis being focused on the Josephson tunneling between such superconductors. The material covered in our previous reviews on the subject concerned [27–31] will be mentioned in brief where necessary, although we decided to avoid repetition as much as possible. We apply our results to cuprates with certain reservations: the actual symmetry of the superconducting order parameter in high-T_c oxides is still not known and the interpretation of the experimental totality is controversial [49–53], although the majority of experts are inclined to believe that cuprates constitute a class of materials with a perfect $d_{x^2-y^2}$-wave symmetry. Hence, our analysis may also be used to indirectly probe the order parameter symmetry. Anyway, the presented theory is quite general and can be applied to other interesting objects.

2. Recent evidence of charge density waves observed in superconductors

In Cu_xTiSe_2, the coexistence between electron-hole and Cooper pairing and the destructive influence of CDW on superconductivity are well established [30,54]. Nevertheless, even the properties of the parent semimetallic layered compound $TiSe_2$ are not properly understood. Even the conventional origin of CDWs in $TiSe_2$ as a consequence of electron-phonon-driven gapping (dielectrization) on the nested Fermi surface (FS) sections [19,23] is contested [54,55]. The failure of the simple basic Peierls scenario is little wonder in view of recent studies of FS in various dichalcogenides revealing much complexity, in particular, strong CDW fluctuations [23,56–61]. However, the competition between dielectric and superconducting instabilities remains a more or less adopted mechanism of their coexistence.

Recently, muon spin rotation and muon spin relaxation measurements were carried out for $Cu_{0.06}TiSe_2$ in the superconducting state, i.e., at the edge of the CDW penetration into the superconducting areal [62]. It turned out that $Cu_{0.06}TiSe_2$ is a single-gap *s*-wave superconductor with the ratio $R \equiv 2\Delta(T=0)/T_c \approx 2.5$, where Δ is the superconducting order parameter, and the Boltzmann constant $k_B = 1$ is adopted throughout the paper. It is much less than the *s*-wave BCS weak-coupling limit $R^s_{BCS} \approx 3.52$. As is well known, any strong-coupling effects lead to the increase of R rather than to its reduction as compared to R^s_{BCS} [63]. We think that the discrepancy can be explained by the assumption made by the authors of Ref. 62 that the London penetration depth is determined by $\Delta(T)$ whatever the CDW-related gap $\Sigma(T)$. It is not the case in the mixed CDW superconducting phase [64,65]. Thus, the results of Ref. 62 should be reinterpreted.

Our reasoning is implicitly supported by the CDW observation in a $Cu_{0.06}TiSe_2$ sample [66]. These authors used scanning tunneling microscopy (STM) and spectroscopy and clearly demonstrated that the amplitude of CDW modulation decreases with Cu doping. Therefore, it would be interesting to measure R for samples near $x = 0.08$, i.e. near the top of the superconducting dome. We expect this ratio to be close to R^s_{BCS}. As for the nature of CDWs in Cu_xTiSe_2, it was recently shown by electron band calculations that they might be, at least partially, induced by Coulomb interaction and have the excitonic-insulator origin [67]. Angle-resolved photoemission spectroscopy (ARPES) studies confirmed this viewpoint for undoped 1*T*-$TiSe_2$ [68] and TiC_xSe_{2-x} with C = S or Te [69].

Intercalation of $TiSe_2$ with Pd leads to more involved results than with Cu. Namely, growing x in Pd_xTiSe_2 forces

its electron system to transform in the following order of states: semimetallic–insulating-normal metallic-superconducting-normal metallic [54,70]. It should be noted that the final decline of superconductivity with overdoping — similar to that in cuprates [71] — may be provoked not only by the FS reconstruction [72,47], which, roughly speaking, changes the electron density of states in the original BCS equation for T_c. Instead, it can also be done owing to the screening of electron-phonon matrix elements [73], i.e., owing to the change of the coupling constant in that equation.

Since transition metal dichalcogenides of the 1*T* polytype usually demonstrate a transition into an insulating state at low enough *T*, superconductivity does not emerge there [23]. Hence, a successful attempt was made to suppress the metal-insulator transition (MIT) by intentional disordering in 1*T*-TaS_2 samples [74]. At $T_c \approx 2.1$ K, the disordered 1*T*-TaS_2 became superconducting against the remaining CDW background. The authors of Ref. 74 claim that the MIT, which is of the Mott (Coulomb correlation) type, inhibits superconductivity, whereas CDWs are not significant. In this connection, it is necessary to recall that CDWs in both excitonic [75] and Peierls [76] insulators are also suppressed by charged impurities (defects) so that they can be substantially weaker in disordered samples.

Doping specimens with Fe turned out to be another way to achieve MIT inhibition in 1*T*-TaS_2 [77]. In 1*T*-$Fe_xTa_{1-x}S_2$, superconductivity appears at $x > 0.01$ and reaches its maximum ($T_c = 2.8$ K) at $x \approx 0.02$, while CDWs persist. The superconducting phase ceases to exist at $x > 0.04$ when charge carriers become localized.

The compound 2*H*-TaS_2 is known to be a superconductor with $T_c \approx 0.8$ K in a CDW containing medium [78]. Recently, a more intricate chiral CDW order was found in 2*H*-TaS_2 samples, which exhibited superconductivity below 1.75 K [79]. CDWs consist of clockwise and counterclockwise modulations, similarly to their counterparts discovered in 1*T*-$TiSe_2$ [80]. The coexistence between chiral CDWs and superconductivity is interesting *per se* in respect to the possible symmetries of the superconducting order parameter.

Momentum-dependent ARPES spectra of 2*H*-$NbSe_2$ — with the highest $T_c \approx 7.3$ K among this class of layered dichalcogenides [78] — were measured and revealed a competition between CDWs and Cooper pairing [81]. The critical temperature T_c is probably so high because most of the FS is left intact when the CDW emerges at $T_d \approx 33.5$ K [82]. It is notable that no direct connection between nesting and CDW emergence was revealed in 2*H*-$NbSe_2$ [81].

Another dichalcogenide, $IrTe_2$, was directly shown using the electron diffraction technique [83] to be a Peierls insulator of the charge-orbital density wave type [84]. The appearance of CDW superlattice peaks correlates with the emergence of resistive and magnetic anomalies at about $T_d = 262$ K. The revealed CDW wave vector agrees well with the theoretical value of FS nesting vector. By intercalation and substitution, samples of Pd_xIrTe_2 ($x > 4\%$) and $Ir_{1-y}PdyTe_2$ ($y > 0.05$) with a fully suppressed orbital CDW were obtained. Therefore, in accordance with the reasoning given in works [85,86], the doped samples become superconducting with T_c up to 3 K.

New data were lately obtained for trichalcogenides as well. Specifically, large attention was attracted to $ZrTe_3$, which exhibits a CDW transition below $T_d \approx 63$ K and is a mixed filamentary-bulk superconductor [87]. Thus, there is a large superconducting tail in the heat capacity and anisotropic resistive *T*-dependences up to higher $T \approx 5$ K, whereas a bulk BCS-like state is stabilized below $T = 2$ K. On the other hand, the intercalation of $ZrTe_3$ with Ag or Cu changes neither T_d nor the onset T_c, but conspicuously reduces the nested FS section area [88,89]. It is quite strange, because the decrease of the dielectrically (by CDWs) gapped (dielectrized) FS section should reduce T_d and consequently raise T_c [30,85,90]. It might happen that the effect does exist, but it is too small to be observed.

Intercalation of $ZrTe_3$ with Ni raises the bulk T_c in the $Ni_{0.05}ZrTe_3$ composition up to 3.1 K, whereas the corresponding T_d falls down to 41 K [91]. Such a behavior agrees with basic theoretical considerations for superconductors partially gapped by CDWs [30,85,90].

Bulk transport and STM measurements in CaC_6 revealed [92] a subtle evidence of CDW formation at $T_d \approx 250$ K, whereas the superconducting T_c in this intercalated graphite compound is rather high (11.5 K) [93]. It would be interesting to influence CDWs to uncover relations between CDWs and superconductivity in this material.

The relationship between superconductivity and CDWs was also studied in pseudoternary alloys $Lu_2Ir_3(Si_{1-x}Ge_x)_5$, $Lu_2(Ir_{1-x}Rh_x)_3Si_5$, and $(Lu_{1-x}Sc_x)_2IrSi_5$ [94]. Magnetic, resistive, and heat-capacity measurements demonstrated that all those materials demonstrate a pronounced anti-correlation between T_d and T_c. Studies of the basic compound $Lu_2Ir_3Si_5$ showed an interesting feature, namely, the coexistence of CDW- and normal-state domains (phase separation) [95]. It resembles the intrinsic nonhomogeneity of CDW gaps in $Bi_2Sr_2CaCu_2O_{8+\delta}$ samples [96]. Unfortunately, the origin of phase separation in those and other substances with CDWs and SDWs is not known for sure, notwithstanding the long history of the problem exploration [97–105].

An interesting CDW superconductor KNi_2Se_2 was recently found. It has a rather low $T_c \approx 0.8$ K and a weak fluctuating CDW at high T which disappears on cooling down at 15 K < *T* < 25 K [106]. These results are unusual and should be checked independently to establish the relations between two kinds of ordering.

NMR and specific-heat measurements revealed that the noncentrosymmetric superconducting carbide Mo_3Al_2C with $T_c \approx 9$ K hosts CDWs below $T_d \approx 130$ K [107]. The CDW gap in the electron density of states is partial and

leaves a sufficient FS section for the subsequent superconducting gapping.

Another way to ensure the coexistence of order parameters in the same material is to spatially separate structural blocks exhibiting CDWs and superconductivity. This possibility was realized in the oxide $Ba_2Ti_2Fe_2As_4O$ leading to a remarkable effect [108]. The layers Fe_2As_2 provide bulk superconductivity with $T_c \approx 21\,\mathrm{K}$, whereas Ti_2O sheets are responsible for the density-wave-induced magnetic and resistive anomalies at $T_d \approx 125\,\mathrm{K}$, which might be of either CDW or SDW origin.

3. Pseudogaps and charge density waves in superconducting cuprates

As we indicated in the Introduction, the ubiquitous pseudogaps should most probably be associated with CDWs. Last years of experimental studies added much to the evidence concerning both manifestations of the same phenomenon — the combined reconstruction of the crystal ion and electron subsystems accompanied by the density of states depletion [48,109–114].

The oxide $Bi_2Sr_2CaCu_2O_{8+\delta}$ is the most typical example of the pseudogap influence on various measured properties and one of the most widely investigated pseudogap-possessing cuprates. The coexistence of pseudogap with superconducting gaps was clearly demonstrated by analyzing the quasiparticle relaxation dynamics in underdoped $Bi_2Sr_2CaCu_2O_{8+\delta}$ samples [115]. Two relaxation processes revealed the following zero-T values of the superconducting gap and the pseudogap: $\Delta(0) \approx 24\,\mathrm{meV}$ and $\Sigma(0) \approx 41\,\mathrm{meV}$, respectively (note that we use our unified notations throughout the paper). Those gap values are in qualitative agreement with $\Delta(0) \approx 28\,\mathrm{meV}$ and $\Sigma(0) \approx 36\,\mathrm{meV}$ found in tunneling experiments for slightly overdoped samples [116]. We emphasize that both Δ and Σ coexist below T_c, which is verified by the time-resolved optical spectroscopic [115,117] and tunnel [41,116,118–120] studies of $Bi_2Sr_2CaCu_2O_{8+\delta}$. Of course, this picture might be oversimplified as compared, e.g., with a complicated phenomenological tripartite model [121], where the checkerboard and pseudogap components are distinct entities. According to the authors of Ref. 121, the model concerned covers all the data obtained for the electron density of states in $Bi_2Sr_2CaCu_2O_{8+\delta}$ [122].

The Nernst coefficient was measured in a wide range of T for the related oxides $Bi_2Sr_{2-x}R_xCuO_y$ (R = La and Eu) and it was shown that the pseudogap component which appears below $T_d > T_c$ develops differently with varying x and R as compared to the superconducting one [123]. Moreover, the pseudogap suppresses superconductivity similarly to its behavior in $Bi_2Sr_2CaCu_2O_2$.

The magnetic torque was studied in $Bi_2Sr_{1.4}La_{0.6}CuO_{6+\delta}$ both above and below $T_c \approx 25\,\mathrm{K}$ [124]. The authors found anisotropic superconductivity below T_c, while above T_c up to $50\,\mathrm{K}$ the anisotropy disappears and Cooper pairs are localized in small regions. The absence of long-range coherence was associated by the authors of Ref. 124 with the destructive action of pseudogap state.

Heavily overdoped compositions of $Bi_2Sr_2CuO_{6+\delta}$ oxide with low and vanishing T_c's were studied by tunneling spectroscopy [125]. The quasiparticle single-peak current-voltage characteristics dI_{qp}/dV were found for certain patches of the surface along with two-peak BCS-like patterns. The single-peak pattern was attributed to the van Hove singularity in the electron spectrum. The spatial path from patch to patch was reflected by the gradual transformation of spectra between two extremes. This picture was observed both in the superconducting state and above T_c so that the gap-related peaks corresponded to pseudogaps. It is remarkable that the superconducting dome was totally surrounded by the pseudogap region in the T–δ phase diagram rather than crossed by the T_d line as, say, in $Bi_2Sr_2CaCu_2O_{8+\delta}$. Thus, the topology of superconducting cuprate phase diagrams turned out to be nonuniversal. As for the van Hove peak, a possible scenario taking it into account together with competing pseudogaps and superconducting gaps was suggested in Ref. 126.

ARPES measurements of $Bi_{1.5}Pb_{0.55}Sr_{1.6}La_{0.4}CuO_{6+\delta}$ oxide directly probed the interplay between Δ and Σ [127]. The results strongly suggest the pseudogap-driven distortion of the *d*-wave superconducting gap in the antinodal region with a more or less *d*-wave-like superconducting gap in the nodal direction. This result agrees well with our model of the competitive coexistence between the CDW gap and the *d*-wave superconducting gap in high-T_c oxides [30–33,128–130].

A viewpoint opposite to ours was expressed based on STM studies of $Ca_{2-x}Na_xCuO_2Cl_2$ ($0.06 \le x \le 0.12$) [131]. Namely, the cited authors traced the doping-induced transition from the antiferromagnetic Mott insulator to the superconductor via the pseudogap state with the C_{2v} unidirectional-symmetry inside clusters surrounded by the original C_{4v} matrix. The clusters start to percolate at $x = 0.08$ when the long-range superconducting order emerges. The authors of Ref. 131 make a conclusion that the pseudogap is beneficial for superconductivity in this substance. It seems, however, that this statement is at least premature. The observed phase separation and superconductivity caused by extra charge carriers can have different microscopic origins. For instance, superconductivity is boosted by the growing electron density, whereas the nonhomogeneous cluster formation and percolation are probably due to the auto localization effects appropriate to the parent magnetic matrix [97].

An important feature of pseudogap manifestations in various high-T_c superconductors is their intrinsic spatial inhomogeneity [30,96,109,131–134] which might be deeply connected to the phase separation discussed above [97–105].

Pseudogaps as actual CDW-gap features in the momentum-dependent energy spectra are accompanied by CDWs

directly vizualized in the co-ordinate space [8,113]. These unidirectional or checkerboard modulations in cuprates usually are fluctuating rather than long-range ones [135,136]. They are also blurred by a random disorder appropriate to bertollides with the intrinsic oxygen nonstoichiometry [137,138]. A superposition of periodicity and disorder of various kinds results in a multi-scale complexity observed, in particular, in $Bi_2Sr_2CaCu_2O_2$ [109,139].

Studies of such CDWs elucidated new facts concerning their relationship with superconductivity. In particular, the $YBa_2Cu_3O_{7-\delta}$ oxide with its CuO chains coupled to CuO_2 layers is a perfect candidate for CDW realization. Indeed, early STM investigations did uncover super-modulations with doping-dependent spatial period [140]. This observation was confirmed by momentum-resolved ARPES measurements that determined the wave-vector $\mathbf{Q}_{CDW} = 2\mathbf{k}_F \approx$ $\approx 0.55\ \text{A}^{-1}$ of the chain CDW [141].

Incommensurate CDW long-range (i.e., up to $(16 \pm 2)a$ at $T \to T_c + 0$, where a is the lattice constant) fluctuations were revealed by resonant x-ray scattering in the CuO_2 plane of $(Y,Nd)Ba_2Cu_3O_{6+x}$ [142]. It turned out that the superconducting state arising at T_c arrests the incipient CDW and prevents the divergence of its correlation length. This is another confirmation of the antagonism between CDWs and Cooper pairing.

3.1. Pnictides and chalcogenides: SDWs or CDWs?

Pseudogaps were also found in the iron-based pnictide $BaFe_2As_2$ by infrared optical conductivity studies [143]. They are similar to those revealed in cuprates but are induced by SDWs rather than CDWs. The ARPES measurements in the underdoped $Ba_{0.75}K_{0.25}Fe_2As_2$ confirmed the pseudogap existence below T_c and its SDW origin [144]. Superconductivity is suppressed by pseudogapping also in the spirit of the struggle for the FS [145].

On the other hand, in the superconducting selenide $K_{0.73}Fe_{1.67}Se_2$ with $T_c \approx 32$ K, the charge density superstructural modulation with the $\sqrt{2} \times \sqrt{2}$ periodicity was found by STM [146]. Possible interference of CDWs into the SDW versus superconductivity competition in iron-based superconductors stems from theoretical considerations as well [147,148].

4. CDW *d*-wave superconductors

4.1. Model parameters

Although the overall T-behavior of the energy gaps is, at first glance, very similar for the isotropic s-wave and d-wave superconductors [149], small distinctions between the behavior of $\Delta(T)$ and $\Sigma(T)$ functions, which are a consequence of the difference between the momentum dependences of those order parameters, become crucial for the interplay between superconductivity and electron-hole dielectric pairing [30–32,128–130]. Thus, the simple situation for the competition between the isotropic order parameters $\Delta(T)$ and $\Sigma(T)$, when only the ratio between the parent pairing strengths determines which state wins [90], is no longer valid.

Here, we restrict ourselves to the scenarios possible for cuprates with their quasi-two-dimensional electron spectrum [72,126,150–152]. In Fig. 1, the geometry of FS gapping by both considered mechanisms is illustrated. The CDW d-wave superconductor is a "child" of two "parents": a d-wave BCS superconductor and a partially gapped CDW metal. Each of them brings about a specific FS gapping that is anisotropic in the momentum space (Fig. 1(a)). We select the bisectrix orientation for the posi-

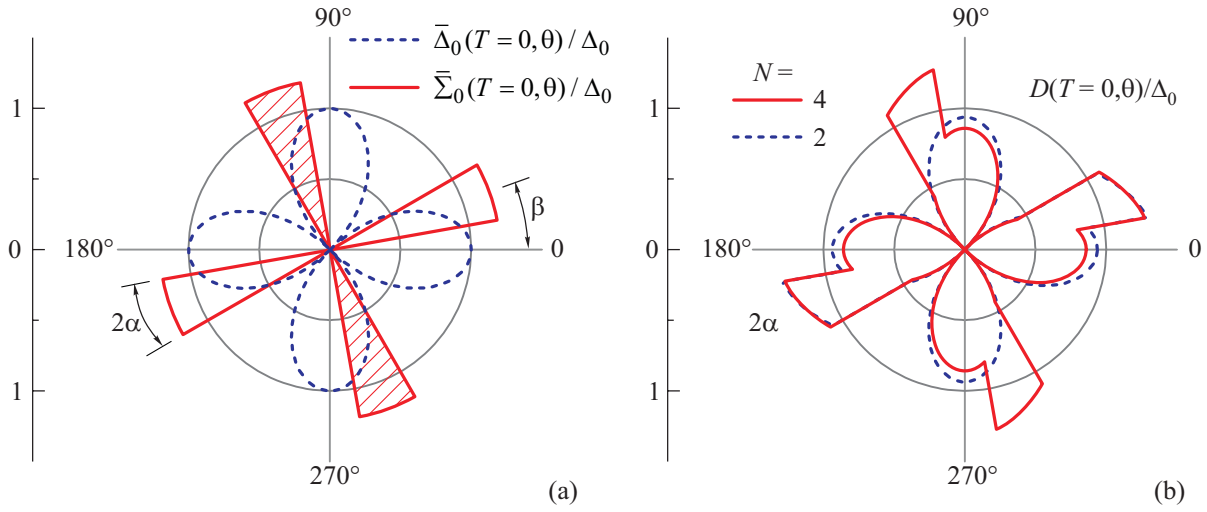

Fig. 1. Order parameter profiles for the parent BCS d-wave superconductor, $\bar{\Delta}_0(\theta)$, and the parent partially gapped CDW metal, $\bar{\Sigma}_0(\theta)$. All four CDW sectors are active for the checkerboard CDW configuration, and only two unhatched sectors remain for the unidirectional one (a). The corresponding gap roses for the checkerboard $(N = 4)$ and unidirectional $(N = 2)$ CDW configurations. The specific calculation parameters are $\sigma_0 = 1.2$, $\alpha = 10°$, $\beta = 20°$, and $T = 0$. See explanations in the text (b).

tive lobe of superconducting order parameter Δ as a reference angle. Then, the actual profile $\overline{\Delta}(T,\theta)$ of superconducting order parameter on the FS of parent superconductor at the temperature T is given by the formula

$$\overline{\Delta}(T,\theta) = \Delta(T) f_{\Delta}(\theta). \tag{1}$$

Here, $\Delta(T)$ is the conventional T-dependence of superconducting order parameter equal to the maximal value of superconducting order parameter lobes, and

$$f_{\Delta}(\theta) = f_{\Delta}^{d}(\theta) = \cos 2\theta \tag{2}$$

is the temperature-independent angular factor for *d*-wave superconductors. We also intend to consider the *s*-extended symmetry of superconducting pairing, for which expression (1) describing the order parameter profile remains valid, but

$$f_{\Delta}(\theta) = f_{\Delta}^{s-\mathrm{ext}}(\theta) = \left|\cos 2\theta\right| \tag{3}$$

in this case, i.e., all the lobes have the same sign (for definiteness, positive).

As was said in Sec. 3, two configurations for CDWs in cuprates are observed, unidirectional and checkerboard. They correspond to two ($N = 2$) or four ($N = 4$), respectively, nested sections arranging in pairs oppositely to each other on the FS. Moreover, in the checkerboard configuration ($N = 4$), the vectors connecting opposite nested sections are mutually perpendicular and experiments testify to the identity of two arising CDWs [30,31]. Therefore, we select the simplest model, when both CDWs are mutually perpendicular and described by the same order parameter $\Sigma(T)$. Formally, the CDW sectors (cones), which confine the dielectrized (d) FS sections, can be oriented arbitrarily with respect to the superconducting lobes. (The nondielectrized FS sections will be denoted as "nd" ones.) To describe this mismatch, we introduce the angle β between the bisectrix of the positive superconducting lobe and the bisectrix of the nearest CDW sector (Fig. 1(a)). We select the simplest model for the FS-profile of the dielectric order parameter Σ in the "parent" CDW metal,

$$\overline{\Sigma}(T,\theta) = \Sigma(T) f_{\Sigma}(\theta), \tag{4}$$

similar to formula (1). Here, $\Sigma(T)$ is the T-dependence of CDW order parameter, and the T-independent profile function $f_{\Sigma}(\theta)$ is defined as equal 1 on the FS *d*-sections and 0 on the *nd*-ones,

$$f_{\Sigma}(\theta) = \begin{cases} 1, & \text{for } \beta - \alpha + k\Omega < \theta < \beta + \alpha + k\Omega, \\ 0, & \text{otherwise}, \end{cases} \tag{5}$$

where k is an integer number, the angle α describes the T-independent parameter describing the FS dielectrization degree (half the opening angle of any of identical CDW sectors), and

$$\Omega = \begin{cases} \pi/2, & \text{for } N = 4, \\ \pi, & \text{for } N = 2. \end{cases} \tag{6}$$

To make the parameter set complete, we add the parameters Δ_0 and Σ_0 associated with the strength of the BCS (electron-electron) or the CDW (electron-hole) pairings, respectively, and equal to the magnitudes of the corresponding "parent" order parameters at $T = 0$, and the number of CDW sectors N.

The relevant system of equations for the order parameter magnitudes $\Delta(T)$ and $\Sigma(T)$ is solved self-consistently [30–32,128–130], because both engaged mechanisms of FS gapping interfere. As a result, a combined gap profile (the gap rose in the momentum space)

$$D(T,\theta) = \sqrt{\overline{\Sigma}^2(T,\theta) + \overline{\Delta}^2(T,\theta)}. \tag{7}$$

appears on the whole FS (see Fig. 1(b)), including the *nd* FS sections, for which $\Sigma(T,\theta) = 0$ (see Eq. (5)) so that $D(T,\theta) = \left|\overline{\Delta}(T,\theta)\right|$ there. Figure 1 clearly demonstrates that the availability of CDWs suppress superconductivity. It can be seen, e.g., from the fact that the magnitude of superconducting lobe on the FS nd sections is reduced in comparison with its "parent" value (cf. both panels), and this reduction is more pronounced for a higher fraction of FS dielectrization at $N = 4$. The reverse detrimental action of superconductivity on CDWs is more intricate (see below).

In what follows, it is convenient to introduce the notation $S_{CDWN}^{\mathrm{sym}\beta}$ for a partially gapped CDW superconductor, which reflects a certain symmetry "sym" of the superconducting order parameter (see below) with the mismatch angle β between the superconducting lobes and CDW sectors, as well as the checkerboard ($N = 4$) or unidirectional ($N = 2$) CDW configuration. In particular, Fig. 1 exhibits the results of calculations for $S_{CDW4}^{d\beta=20^\circ}$ and $S_{CDW2}^{d\beta=20^\circ}$ CDW superconductors. The special case of *d*-wave symmetry with $\beta = 0^\circ$, as for cuprates, will be denoted in the conventional manner $d_{\beta=0^\circ} = d_{x^2-y^2}$. For the hypothetical case $d_{\beta=45^\circ}$, which we also intend to analyze, the corresponding notation is d_{xy}. All intermediate β values might be possible only in the case of internal deformations, when the crystal symmetry inherent to cuprates is broken; it will not be analyzed below. As was indicated in the Introduction, we shall also consider the cases of extended *s*-wave symmetry for the superconducting order parameter, for which we shall use the notations $s_{x^2-y^2}^{\mathrm{ext}}$ and s_{xy}^{ext}. We also introduce the notations S_{BCS}^{s} and S_{BCS}^{d} for "pure" *s*- and *d*-wave superconductors, respectively.

The number of energy-dependent parameters of the problem is reduced by normalizing them by the parameter Δ_0. Thus, we introduce the dimensionless parameter $\sigma_0 = \Sigma_0/\Delta_0$ describing the relative strength of the CDW and BCS pairings, the dimensionless temperature $t = T/\Delta_0$, and the dimensionless order parameters $\sigma(t) = \Sigma(T)/\Delta_0$ and $\delta(t) = \Delta(T)/\Delta_0$.

4.2. Phase diagrams

Bearing in mind the discrete sets of allowed values for the parameters N (2 and 4) and β (0 and 45°), it is natural to construct phase diagrams on the plane of continuous variables α and σ_0 [31,32]. Figure 2 exhibits the phase diagrams for both the checkerboard and unidirectional CDW geometries. The small-α ($0° < \alpha < 45°$) half of the diagram for the case $N = 2$ almost exactly reproduces the total diagram for the case $N = 4$ [32]. The difference consists in the following. The pure CDW phase (denoted by bold lines) is possible only at $\sigma_0 > \bar{\sigma}_0 = \sqrt{e_N}/2$, where $e_N \approx 2.718...$ is Napier's constant, and provided that the total FS dielectrization takes place. The latter corresponds to $\alpha = 45°$ for the checkerboard and $\alpha = 90°$ for the unidirectional CDW configuration. Each solid curve divides the plane $\alpha - \sigma_0$ into the pure BCS (to the left) and BCS + CDW (to the right) areas. The partially dielectrized phase is supposed to be inherent for cuprates ($\beta = 0°$) and corresponds to the ubiquitous state of high-T_c oxides with pseudogaps. Their presence may, however, be hidden because of the spatially nonhomogeneous pseudogap distribution [30,96,109,131]. Nevertheless, the pseudogap features can be clearly seen as smeared dip-hump features in cuprate tunnel spectra [119,132,133,153].

There is also important indirect evidence that CDW-driven pseudogaps do exist. We mean the anomalously large values of the ratio $5.5 \le R \le 13$ for various cuprates [71,154].The same is true for iron-based pnictides and

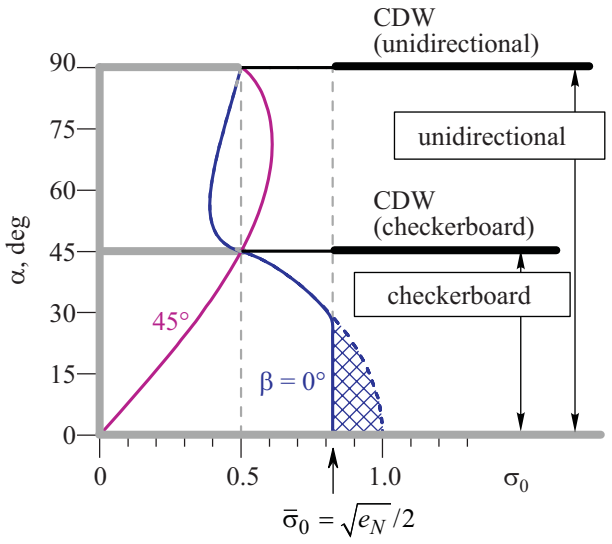

Fig. 2. Calculated phase diagrams for $S^{d_{x^2-y^2}}_{CDW4}$ and $S^{d_{x^2-y^2}}_{CDW2}$ superconductors ($\beta = 0°$), as well as $S^{d_{xy}}_{CDW4}$ and $S^{d_{xy}}_{CDW2}$ ones ($\beta = 45°$). The gray boundaries correspond to the pure BCS *d*-wave superconductor, and the bold black ones to the pure CDW metal. The horizontal boundary at $\alpha = 45°$ is actual only for the checkerboard CDW configuration. See other notations and explanations in the text.

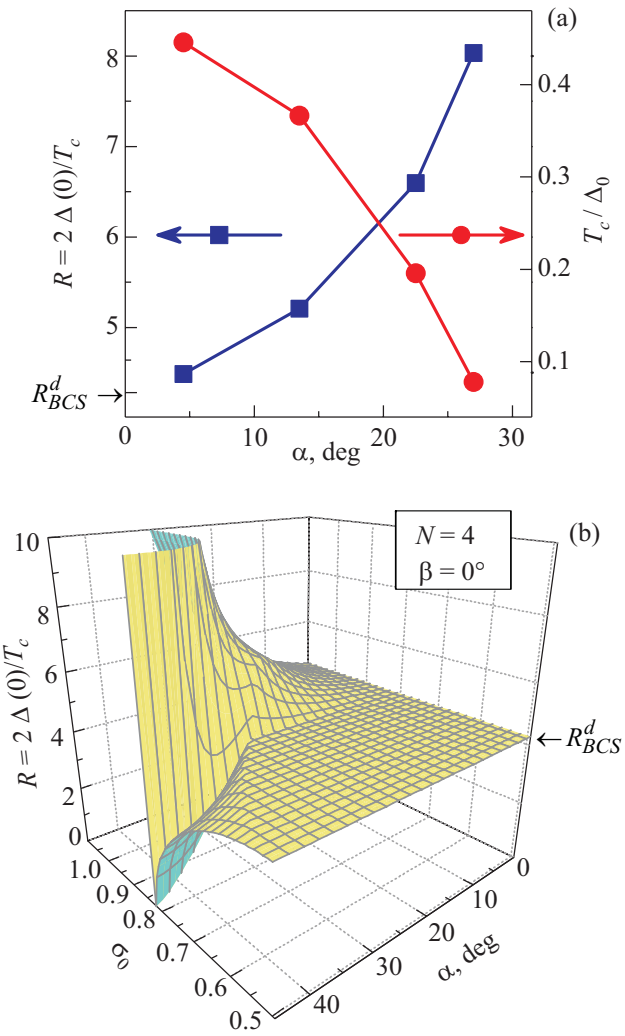

Fig. 3. Dependences of the quantities $R = 2\Delta(0)/T_c$ and T_c/Δ_0 on the parameter α for $S^{d_{x^2-y^2}}_{CDW4}$ with $\sigma_0 = 1$ (a). 3D map $R(\Delta_0, \alpha)$ for $S^{d_{x^2-y^2}}_{CDW4}$ (b).

chalcogenides [154]. The observed values of the ratio strongly exceed the weak-coupling *s*- and *d*-wave universal numbers R^s_{BCS} and $R^d_{BCS} \approx 4.28$, respectively. Strong-coupling effects alone [155] cannot explain such a huge discrepancy with weak-coupling theories [40,154]. On the other hand, the CDW influence, which reduces, but non-uniformly, both the $\Delta(0)$ and T_c magnitudes, is capable of explaining the experimental results [128]. Figure 3(a) illustrates how the ratio R increases with the growth of α. Note that this increase is accompanied by a rapid reduction of T_c. This correlation qualitatively agrees with the behavior of underdoped cuprate compositions with extremely high R's and reduced T_c's as compared with optimally doped samples. The approximate proportionality between R and T_c [154] does not work here. Figure 3(b) exhibits the variation of the ratio R in a wider range of parameters σ_0 and α, for which Fig. 3(a) is a cross-section. One can see that R can acquire not only values that substantially

exceed the R^d_{BCS} constant, but it also can decrease as compared to this value, even down to zero (!), although in rather a narrow parameter range. As for Fe-based superconductors, their high R values [154] might be connected to the coexisting superconductivity and SDWs [147,156]. The detrimental action of the latter on the former is very similar to the influence of CDWs on superconductivity analyzed in this work. However, the corresponding calculations have not been made yet.

In Fig. 2 one can see a hatched region with peculiar properties, namely the T-reentrance of CDW dielectric order parameter. This region exists if $\beta = 0°$, but is absent if $\beta = 45°$. This phenomenon is caused by a slightly different steepness of $\Delta(T)$-dependences for s- and d-wave mean-field BCS order parameters (whatever their microscopic origin) [129,130]. As a consequence, it may happen that, for certain parameter values, the distortion of $\Sigma(T)$ by its $\Delta(T)$ counterpart leads to the total suppression of Σ in a T-range from zero up to a certain temperature T_r, i.e., in essence, to the disappearance of CDWs in this T-interval [32]. This predicted phenomenon remains to be found experimentally. In the case of unidirectional CDWs ($N = 2$), the α-reentrance of Σ should also take place, as can be seen from Fig. 2.

5. Josephson tunneling through junctions involving CDW *d*-wave superconductors

The coexistence between the order parameters of different symmetries and the reentrance behavior should inevitably influence the Josephson current in junctions involving CDW superconductors with d- or extended s-wave pairing symmetry.

5.1. Theory

Owing to the quasi-two-dimensional character of the FS for high-T_c oxides, the simplest geometry of the tunnel junction between such two superconductors is chosen. Namely, the c-axes of the both are assumed to be parallel to each other and to the junction plane.

In the tunnel Hamiltonian approach, the dc Josephson critical current through a tunnel junction between two superconductors, whatever their order parameter symmetry, is given by the general equation

$$I_c(T) = 4eT\sum_{\mathbf{pq}}\left|\tilde{T}_{\mathbf{pq}}\right|^2 \sum_{\omega_n} \mathrm{F}^{+}(\mathbf{p};\omega_n)\mathrm{F}'(\mathbf{q};-\omega_n), \qquad (8)$$

Here, $\tilde{T}_{\mathbf{pq}}$ are the matrix elements of tunnel Hamiltonian; they correspond to various combinations of FS sections for superconductors taken on different sides of tunnel junction; $\mathbf{p}$ and $\mathbf{q}$ are the transferred momenta; $e > 0$ is the elementary electrical charge, and $\mathrm{F}(\mathbf{p};\omega_n)$ and $\mathrm{F}'(\mathbf{q};-\omega_n)$ are Gor'kov Green's functions for superconductors to the left and to the right, respectively, of the tunnel barrier (the primed quantities will be associated with the r.h.s. electrode). The internal summation is carried out over the discrete fermionic "frequencies" $\omega_n = (2n+1)\pi T$, $n = 0, \pm1, \pm2, \ldots$. The external summation takes into account the possible anisotropy of electron spectra $\xi(\mathbf{p})$ and $\xi'(\mathbf{q})$ in both superconductors in the manner suggested long time ago for all kinds of anisotropic superconductors [157], the directionality of tunneling [158,159], and the dielectric electron-hole (CDW) gapping of the nested FS sections (if any) [160]. Let us assume for definiteness that $\mathrm{F}(\mathbf{p};\omega_n)$ corresponds to a high-T_c oxide superconductor (CDW gapped, in the general case) with a d-wave or an extended s-wave order parameter ($S^{\mathrm{sym}}_{\mathrm{CDW}N}$ in our notation). At the same time, $\mathrm{F}'(\mathbf{q};\omega_n)$ may correspond to either the same high-T_c oxide (S^{sym}_{CDWN}) or an s-wave isotropic superconductor of the original BCS model (S^{s}_{BCS}) with the order parameter $\overline{\Delta}_{sBCS}(T)$ [40]. Thus, we restrict ourselves to two representative cases: (i) a junction involving identical high-T_c superconductors, i.e., the symmetrical setup $S^{\mathrm{sym}}_{CDWN} - I - S^{\mathrm{sym}}_{CDWN}$, and (ii) a nonsymmetrical one, $S^{\mathrm{sym}}_{CDWN} - I - S^{s}_{BCS}$. In both cases, the parameter "sym" will be varied. The expressions for relevant Green's functions can be found elsewhere [33].

As an example, Fig. 4 illustrates both those cases if the CDW superconductor to the left (and to the right in the symmetrical case) is $S^{d_{x^2-y^2}}_{CDW4}$. We consider the gap rose of the CDW superconductor to the left from the junction plane to be oriented at an angle γ with respect to the normal to the plane. Note that the orientation direction of the whole CDW d-superconductor is defined as that of the bisectrix of the positive superconducting order parameter lobe. The gap rose of the superconductor to the right from the junction is, in the general case, oriented at a different angle, γ', with respect to the normal. For the nonsymmetric junction geometry, the gap rose of the r.h.s. superconductor (S^{s}_{BCS}) is an isotropic circle.

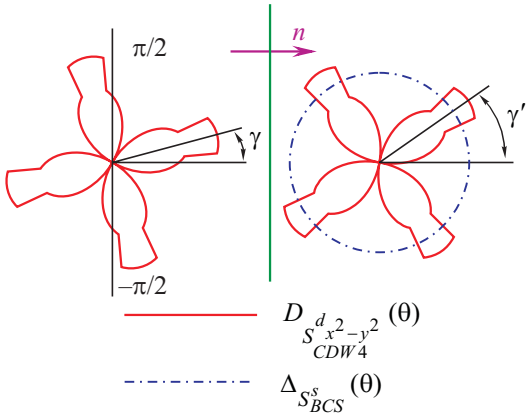

Fig. 4. Orientations of gap roses in both electrodes with respect to the normal $\mathbf{n}$ to the junction plane for the symmetrical, $S^{d_{x^2-y^2}}_{CDW4} - I - S^{d_{x^2-y^2}}_{CDW4}$, and nonsymmetrical, $S^{d_{x^2-y^2}}_{CDW4} - I - S^{s}_{BCS}$, junction configurations.

Specifying the dc Josephson current (8), we introduce two kinds of directionality. The first one involves the factors $\left|\mathbf{v}_{g,nd}\cdot\mathbf{n}\right|$ and $\left|\mathbf{v}_{g,d}\cdot\mathbf{n}\right|$ [161,162], where $\mathbf{v}_{g,nd}=\nabla\xi_{nd}$ and $\mathbf{v}_{g,d}=\nabla\xi_{d}$ are the quasiparticle group velocities for proper FS sections. Those factors can be considered as proportional to the number of electron attempts to penetrate through the barrier [163]. In the framework of the phenomenological approach adopted here, this multiplier can be factorized into $\cos\theta$, where θ is the angle at which the pair/quasiparticle penetrates through the barrier, and an angle-independent coefficient, which can be in the usual way incorporated into the junction normal-state resistance R_N (see below).

In addition, in agreement with previous studies [158,164], the tunnel matrix elements $\tilde{T}_{\mathbf{pq}}$ in Eq. (8) should also make allowance for the tunnel directionality (the angle-dependent probability of penetration through the barrier) [33,161,162,165]. For instance, if the tunnel barrier is considered a finite-width rectangle, the tunnel probability becomes much higher for the particles moving perpendicular to the barrier plane [165]. Since we do not know the actual dependences for realistic junctions from microscopic considerations, we, shall hereafter simulate the barrier-associated directionality as the *n*-th power of $\cos\theta$. In specific calculations, we put $n = 2$.

Substituting corresponding expression for Green's functions into Eq. (8), carrying out standard transformations [1], assuming the coherent character of tunneling described, e.g., in Refs. 50, 158, 165, as opposed to the noncoherent approximation [166,167] valid for isotropic superconductors, and making some simplifications, we obtain the following formula for the dc Josephson current across the symmetrical or nonsymmetrical tunnel junction:

$$I_c(T,\gamma,\gamma') = \frac{1}{2eR_N}\frac{1}{\pi}\int\limits_{-\pi/2}^{\pi/2} d\theta\cos\theta\, W(\theta)\, P(T,\theta,\gamma,\gamma'), \qquad (9)$$

where (cf. Refs. 157, 160)

$$P(T,\theta,\gamma,\gamma') = \overline{\Delta}(T,\theta-\gamma)\overline{\Delta}'(T,\theta-\gamma')\times \int\limits_{\min\{D(T,\theta-\gamma),D'(T,\theta-\gamma')\}}^{\max\{D(T,\theta-\gamma),D'(T,\theta-\gamma')\}} dx\tanh\frac{x}{2T}\times \frac{1}{\sqrt{\left(x^2-D^2(T,\theta-\gamma)\right)\left(D'^2(T,\theta-\gamma')-x^2\right)}}. \qquad (10)$$

As before, the primed quantities are associated with the r.h.s. electrode. The parameter R_N is the normal-state resistance of the tunnel junction determined by $\left|\tilde{T}_{\mathbf{pq}}\right|^2$ without the factorized multiplier $W(\theta)$. Integration over the angle variable θ is carried out within the interval $-\pi/2\le\theta\le\pi/2$, i.e., over the "FS semicircle sections" turned towards the junction plane. As was also indicated above, we put $W(\theta)=\cos^2\theta$ in subsequent calculations. Formula (9) was obtained in the weak-coupling approximation [166], i.e., the reverse influence of the energy gaps on the initial FS was neglected.

At $W(\theta)\equiv 1$ (the tunneling directionality associated with the θ-dependent barrier transmittance is neglected), when putting $f_{\Delta}^{(')}=1$ (actually, it is a substitution of an isotropic *s*-superconductor for the *d*-wave or extended *s*-wave ones) and $f_{\Sigma}^{(')}=0$ (the absence of CDW-gapping), as well as substituting $\cos\theta$ by 1 (the absence of tunnel directionality), Eq. (9) expectedly reproduces the famous Ambegaokar–Baratoff result for tunneling between conventional *s*-wave superconductors [1,166,167] On the other hand, if the directionality and dielectric gapping are excluded, but f_{Δ} and $f_{\Delta}^{'}$ are retained, we arrive at the Sigrist–Rice model [168]. Note, that we restricted ourselves to the classical tunnel junction [166,1], which is a strong-barrier limit of a more general model [169]. It means that Andreev-Saint-James reflection processes [9,170–172] were disregarded.

In this paper, we do not consider the *T*-dependences of Josephson current, leaving this problem to be tackled in a separate paper. Our main goal here is to analyze whether it is possible to determine the type of superconducting pairing in high-T_c oxides, which we regard as CDW *d*- or extended *s*-wave superconductors. Therefore, all further calculations will be carried out for the zero temperature, $T = 0$. We also introduce the dimensionless Josephson current $i_c = (2eR_N/\Delta_0^2)I_c(T=0)$.

6. Josephson tunneling. Results and discussion

Symmetrical Josephson junctions of the $S^{\mathrm{sym}}_{CDWN}-I-S^{\mathrm{sym}}_{CDWN}$ type demonstrate more diversified characteristics due to the availability of a larger number of problem parameters and their possible combinations as compared to the nonsymmetrical $S^{\mathrm{sym}}_{CDWN}-I-S^{s}_{BCS}$ case. Hence, let us begin with the symmetrical case.

6.1. Symmetrical junctions. CDW-governed dependences

The relevant electrode parameters are $\alpha=\alpha'$, $\beta=\beta'$, $N=N'$, $\sigma_0=\sigma'_0$, and (in the general case) $\gamma\ne\gamma'$. To elucidate the effects induced by CDW parameters, let us put $\gamma=\gamma'=0$.

As was shown earlier [160,173] for competing *s*-wave superconductivity and CDWs, the growth of each of the parameters Σ_0 and α of CDW gapping, which is detrimental for superconductivity, results in a suppression of the Josephson tunnel current magnitude. The same should be true for the considered case of *d*-wave superconductors. Indeed, this is demonstrated in Fig. 5 for the symmetrical $S^{d_{x^2-y^2}}_{CDW4}-I-S^{d_{x^2-y^2}}_{CDW4}$ junction with $\gamma=\gamma'=0$. It is instructive to compare both panels with the phase diagram

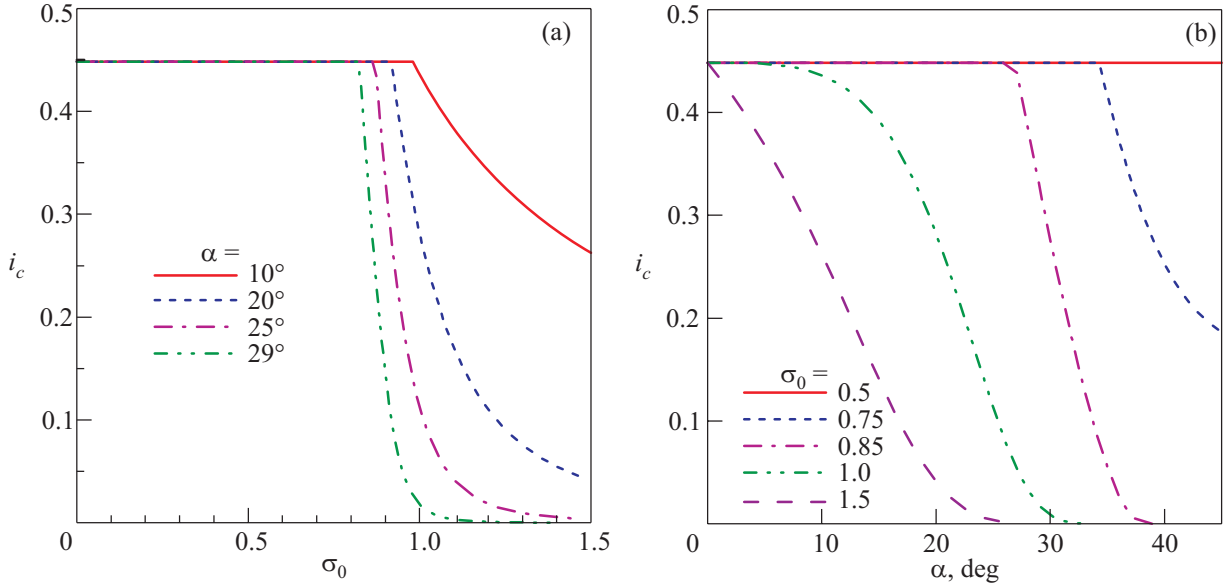

Fig. 5. Dependences of the dimensionless Josephson tunnel current i_c (a) on σ_0 at various α and (b) on α at various σ_0 for the symmetrical $S^{d_{x^2-y^2}}_{CDW4} - I - S^{d_{x^2-y^2}}_{CDW4}$ junction with $\gamma = \gamma' = 0$.

for $\beta = 0°$ in Fig. 2. The curves presented in each of the panels correspond to the phase diagram scanning along either the σ_0- or a-axis. The horizontal sections of the curves correspond to the S^d_{BCS} state of electrodes. If $\alpha = 45°$ (the full FS dielectrization), the states with $\sigma_0 > \bar{\sigma}_0$ are a pure CDW nonsuperconducting metal so that the current i_c in Fig. 5(b) vanishes for them.

Since the results of the interplay between CDWs and superconductivity depends on the degree of overlapping between superconducting lobes and CDW sectors, it is of interest to carry out the same estimations for the case when both electrodes are CDW d_{xy}-wave superconductors ($\beta = 45°$), i.e., for the $S^{d_{xy}}_{CDW4} - I - S^{d_{xy}}_{CDW4}$ junction. The corresponding results are depicted in Fig. 6. They testify that the detrimental action of CDWs on superconductivity is weaker in this case and the relevant dependences are smoother, which could be observed experimentally.

The both figures demonstrate that the growth of each of the CDW-related control parameters σ_0 and α inhibits the superconducting coherent current. Their cumulative

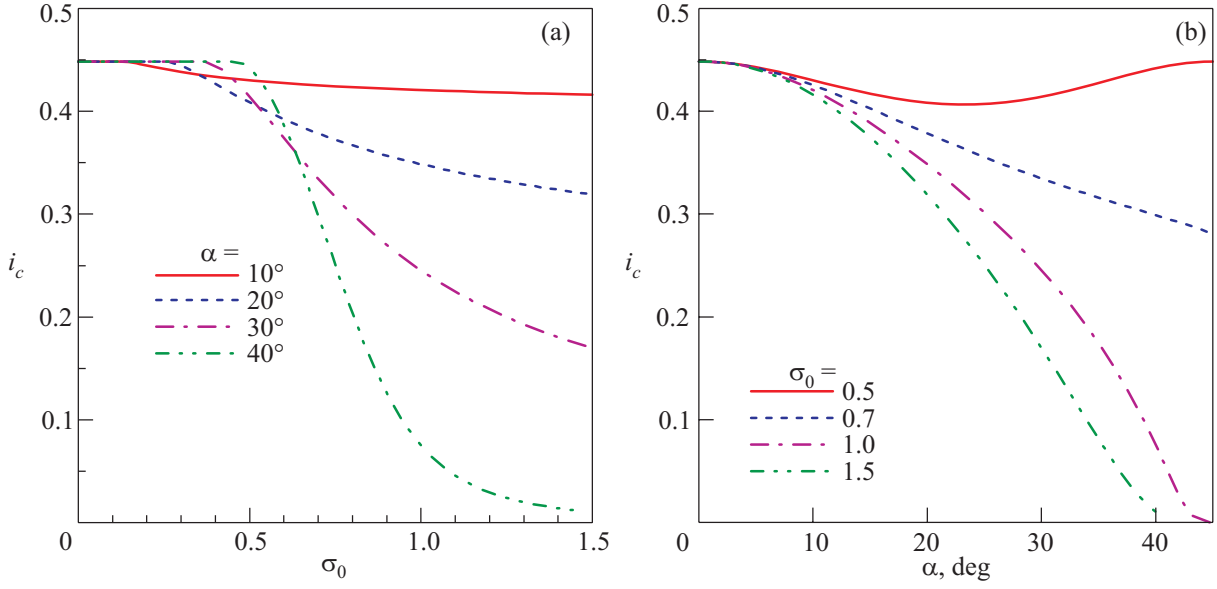

Fig. 6. The same as in Fig. 5, but for the symmetrical $S^{d_{xy}}_{CDW4} - I - S^{d_{xy}}_{CDW4}$ junction.

action also expectedly and effectively reduces the magnitude of the Josephson current through the tunnel junction. Moreover, the significant drop of the calculated Josephson current with the increase of either α or Σ (or the both) correlates well with the observed doping dependence of the currents across mesa structures of $Bi_2Sr_2CaCu_2O_2$ with the intrinsic Josephson inter-layer coupling [120]. For instance, the pseudogap at $T > T_c$ [$2\Sigma(T > T_c)$, in our notations] changes from 131 ± 9 meV for the sample with an average number of holes per Cu atom $p = 0.126$ and $T_c \approx 74.9$ K to (71 ± 11) meV for the sample with $p = 0.186$ and $T_c \approx 78.2$ K. At the same time, the critical Josephson current at $T = 10$ K changes from 0.561 to 4.69 kA / cm^2. One should note that both the CDW sector width and the amplitude of dielectric gap vary from sample to sample in such experiments, as is known from the totality of measurements concerning $Bi_2Sr_2CaCu_2O_{8+\delta}$ including ARPES, STM and break-junction investigations [13,30–32,48,71, 116,119,174–186].

Attention is attracted by the nonmonotonic $i_c(\alpha)$-dependence for $\sigma_0 = 0.5$ in Fig. 6(b). A comparison with the phase diagram for $\beta = 45°$ in Fig. 2 shows that it is a result of electrode transformation into the pure S^d_{BCS} state. To a great extent, it is connected with the crossing of the solid curve in the phase diagram that separates pure BCS and BCS + CDW states. Figure 2 demonstrates that, in the case of unidirectional CDW configuration and in a certain vicinity of $\sigma_0 = 0.5$, such a crossing is quite possible. Therefore, let us consider the corresponding $i_c(\alpha)$-dependences (Fig. 7).

In the case of $S^{d_{x^2-y^2}}_{CDW2} - I - S^{d_{x^2-y^2}}_{CDW2}$ junction (Fig. 7(a)), CDWs are absent at small α's so that the current is constant, then the phase boundary with the reentrant region is crossed and the current starts to decrease with α. After reaching a σ_0-dependent minimum the current begins to grow finally approaching the initial value for $\sigma_0 = 0.45$ or 0.5. However, if the value σ_0 exceeds 0.5 the restoration of i_c is incomplete since in this case the reentrance ceases to exist. Nevertheless, the ascending branch of $i_c(\alpha)$ survives testifying to the proximity to the singular point ($\alpha = 90°$, $\sigma_0 = 0.5$). Thus, measurements of the Josephson current amplitudes may also serve as a probe of the CDW appearance in the superconducting state.

For hypothetical $S^{d_{xy}}_{CDW2}$-superconductors, the situation is in some sense opposite (Fig. 7(b)). According to the phase diagram with $\beta = 45°$ in Fig. 2, small α's correspond to the $S^{d_{xy}}_{CDW2}$-phase. With growing α, the CDW destructive influence on superconductivity starts to increase, which can be seen in Fig. 7(b) as a reduction of i_c. But for large enough α's, the vertical path (σ_0 is kept constant!) on the phase plane approaches the boundary with the pure superconducting S^d_{BCS} phase so that i_c counter-intuitively begins to increase tending to the plateau value. This is true for $\sigma_0 = 0.45$ and 0.5. On the other hand, when $\sigma_0 > 0.5$ ($\sigma_0 = 0.55$ in 7(b)), Σ reappears in the neighborhood of $\alpha = 90°$ (the inverse reentrance as compared to that for $\beta = 0°$), and the current i_c rapidly drops.

6.2. Symmetrical junctions. Angular dependences

Now, consider the angular dependences of tunnel current describing the influence of different crystal orientations relatively to each other and to the junction plane. In this paper, we confine the consideration to the case when the orientation of the r.h.s. electrode with respect to the junction plane is fixed ($\gamma' = 0$, see Fig. 4).

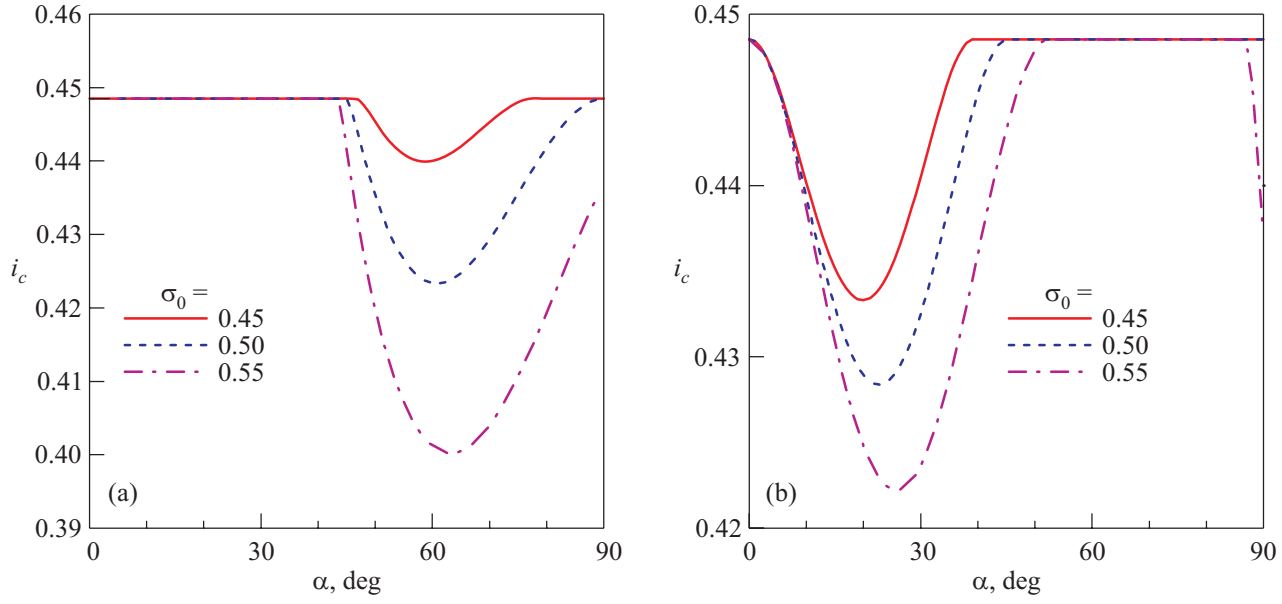

Fig. 7. Dependences of i_c on α at various σ_0 for the symmetrical (a) $S^{d_{x^2-y^2}}_{CDW2} - I - S^{d_{x^2-y^2}}_{CDW2}$ and (b) $S^{d_{xy}}_{CDW2} - I - S^{d_{xy}}_{CDW2}$ junctions with $\gamma = \gamma' = 0$.

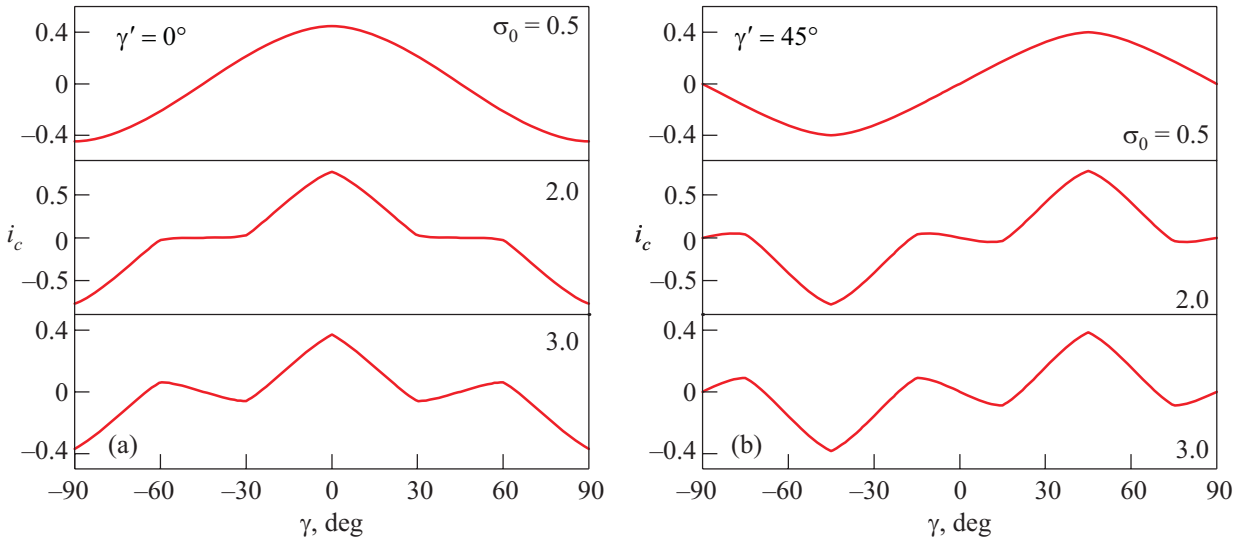

Fig. 8. Dependences of i_c for the symmetrical junction between $S^{d_{x^2-y^2}}_{CDW4}$ electrodes with $\alpha = 15°$ and various σ_0's on the l.h.s.-electrode orientation γ for the fixed orientation of the r.h.s. electrode $\gamma' = 0$ (a) and 45° (b).

In Fig. 8, the curves $i_c(\gamma)$ are presented for $S^{d_{x^2-y^2}}_{CDW4}$ electrodes with a fixed α and varying CDW amplitudes σ_0. This set of parameters approximately corresponds to a high-T_c oxide with varying doping level. The approximation of this compliance, as has already been indicated, consists in the impossibility of changing Σ and leaving α intact. Nevertheless, as follows from the large body of experimental data, the pseudogap onset temperature and the pseudogap magnitude change more rapidly than the corresponding CDW-sector width, thus making our interpretation plausible. Anyway, the influence of σ_0 severely distorts the standard periodic curve appropriate to $d_{x^2-y^2}$-superconductors. Namely, the considered set-up symmetry results in the complete compensation of contributions from elementary Josephson 0- and π-junctions at $\gamma = 45°$ for CDW-free compositions [9]. As one sees from Fig. 8(a), the growing σ_0 first creates wide plateaux in the neighborhood of $\gamma = 45°$. When σ_0 becomes large enough, we arrive at three ascending and three descending sections in the $i_c(\gamma)$-dependence in the range $(-90°, +90°)$ instead of the initial one ascending and one descending branch. If the crystal on the r.h.s. of the junction is rotated by 45° with respect to the normal **n** and the dependence $i_c(\gamma)$ is calculated for the same parameters, the results are different (see Fig. 8(b)). The difference consists not only in the shift of the whole dependence by 45°, but also in its less smooth character, so that the curve may even change its slope sign within certain sections at certain parameters.

As is clear from the aforesaid, the control CDW parameter α should affect the angular dependences of the tunnel current. The corresponding plots are exhibited in Fig. 9. We see that the i_c-magnitude is suppressed by growing α, whereas the dependence $i_c(\gamma)$ itself becomes complicated, similarly to what was observed in Fig. 8.

As was discussed above, CDWs in cuprates are either checkerboard-like or unidirectional ones. It is clear that the gap rose $D(T,\theta)$, which together with the profile $\bar{\Delta}(T,\theta)$ determines the angular dependence of i_c (see Eq. (10)), is "more anisotropic" in the latter case. The "checkerboard" gap rose has the four-fold symmetry, whereas the "unidirectional" pattern has only the two-fold one (see Fig. 1(b)). Therefore, the angular dependences for symmetric junctions composed of S^{d}_{CDW2} electrodes must be more pronounced that those for S^{d}_{CDW4} ones with identical other parameters. The corresponding results are compared in

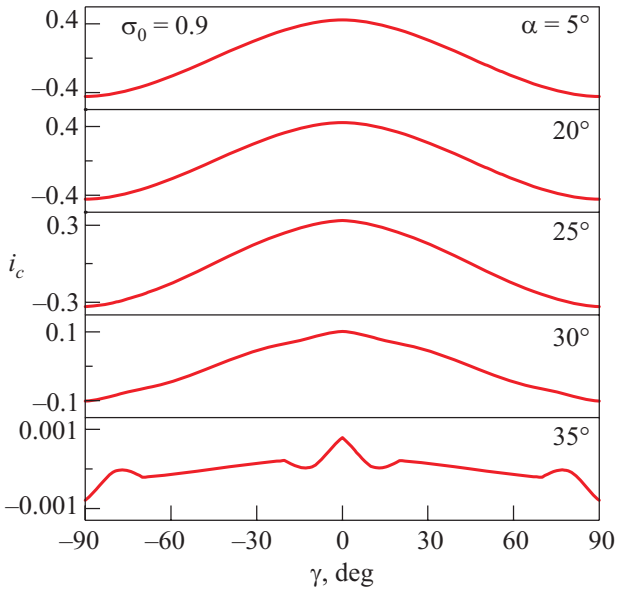

Fig. 9. Dependences of i_c for the symmetrical junction between $S^{d_{x^2-y^2}}_{CDW4}$ electrodes with a fixed σ_0 and various α's on the l.h.s.-electrode orientation γ. The orientation of the r.h.s. electrode is fixed, $\gamma' = 0$.

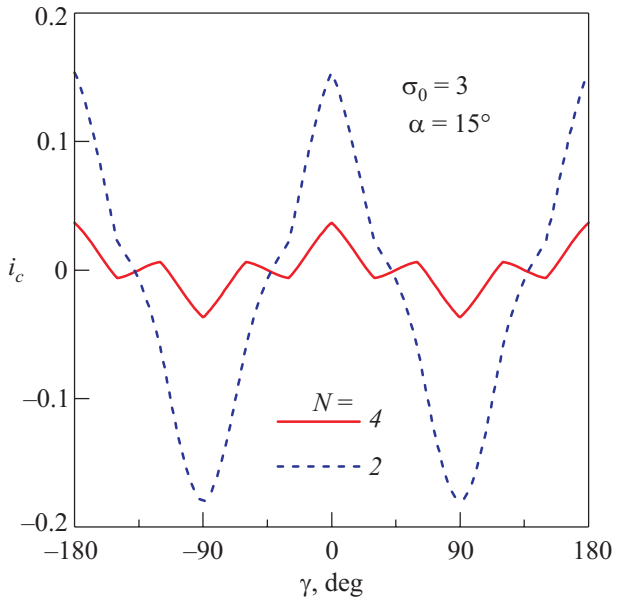

Fig. 10. Dependences of i_c on the l.h.s.-electrode orientation γ for the symmetrical junction between $S^{d_{x^2-y^2}}_{CDW4}$ or $S^{d_{x^2-y^2}}_{CDW2}$ electrodes with $\sigma_0 = 3$ and $\alpha = 15°$. The orientation of the r.h.s. electrode is fixed, $\gamma' = 0$.

Fig. 10. It is readily seen that the appearance of "additional" CDW sectors enhances FS dielectrization so that the amplitude of i_c oscillations expectedly decreases. At the same time, the "checkerboard" dependence turns out "more structured", because the oscillations produced by both superconducting lobes and CDW sectors become more observable.

Oscillations in the $i_c(\gamma)$ dependence stem from the sign alternation of superconducting lobes in the case of *d*-wave pairing symmetry. Therefore, it is also instructive to compare critical currents across junctions involving superconductors with other possible order parameter symmetries. The results of such a comparison are shown in Fig. 11 for symmetrical junctions S^{sym}_{CDW2} electrodes, where the parameter sym = $d_{x^2-y^2}$, $s^{ext}_{x^2-y^2}$, and *s* in panel (a), and sym = d_{xy}, s^{ext}_{xy}, and *s* in panel (b). In the case of *s*-wave symmetry, we need to introduce the orientation parameter γ_{CDW} for CDW sectors, because the superconducting order parameter is isotropic In all three cases in each panel, the orientations of CDW sectors with respect to the junction plane are identical, being fixed for the r.h.s. electrode. The unidirectional CDW configuration was selected, because in the d_{xy}-cases nonsymmetrical $i_c(\gamma)$ dependences are obtained. The figure demonstrates that $i_c(\gamma)$ dependences are very sensitive to the type of superconducting pairing symmetry. Hence, should such an experimental setup be possible, it could provide information concerning not only the pairing symmetry, but also the CDW configuration (checkerboard or unidirectional).

6.3. Nonsymmetrical junctions

In this case, the isotropic weak-coupling BCS superconductor S^s_{BCS} on the r.h.s. of the $S^{sym}_{CDWN} - I - S^s_{BCS}$ junction is characterized by a single dimensionless isotropic parameter $\delta_{BCS} = \Delta^*(T = 0)/\Delta_0$ (see Fig. 4). Its magnitude is assumed to be 0.1 throughout this section, which roughly corresponds to the ratio between the gaps in Nb (the r.h.s. electrode) and, say, $Bi_2Sr_2CaCu_2O_{8+\delta}$ or $YBa_2Cu_3O_{7-\delta}$ taken as the left hand side electrode.

Let us first consider the anomalous behavior of $i_c(\alpha)$ in the reentrance phase-space $(\sigma_0 - \alpha)$ region of the left electrode. In Fig. 12 the currents through the junction between the $S^{d_{x^2-y^2}}_{CDW2}$ (a) or $S^{d_{xy}}_{CDW2}$ (b) on the l.h.s. and the S^s_{BCS} electrodes on the r.h.s. of the junction are shown for various σ_0's. The dependences are similar to those depicted in Fig. 7 for symmetrical junctions with the identical parameters for both S^{sym}_{CDW2} electrodes. At the same time, the current amplitudes are essentially smaller due to the smallness of parameter $\delta_{BCS} = 0.1$.

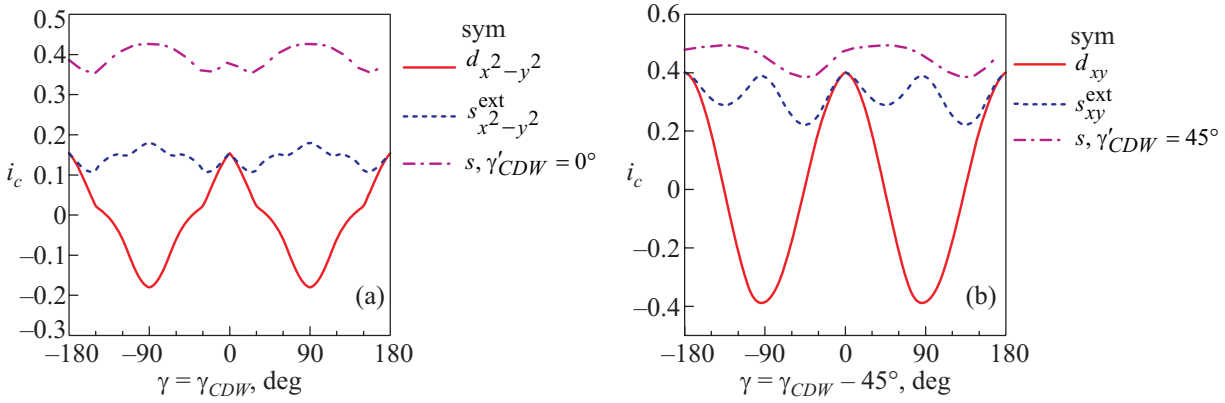

Fig. 11. γ-dependences of i_c for the symmetrical junction between S^{sym}_{CDW2} electrodes with $\sigma_0 = 3$, $\alpha = 15°$, and various symmetries of superconducting order parameter. The orientation of the r.h.s. electrode is fixed, $\gamma' = 0$, with $\gamma' = \gamma'_{CDW}$ in panel (a) and $\gamma' = \gamma'_{CDW}$ — 45° in panel (b). See explanations in the text.

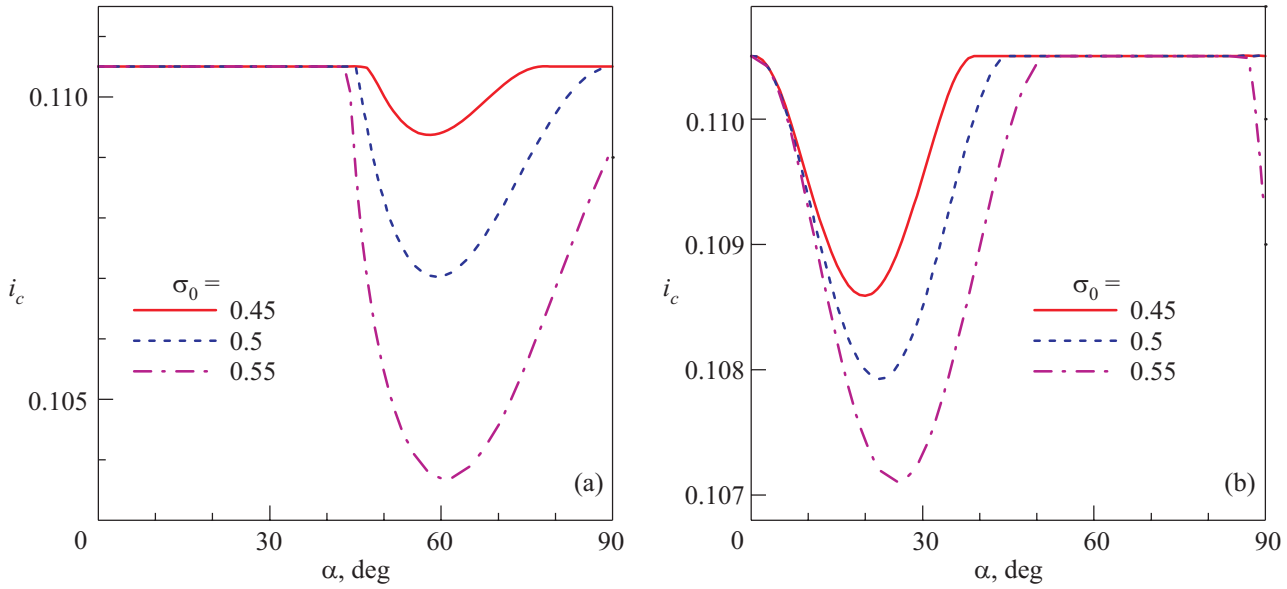

Fig. 12. The same as in Fig. 7, but for the non-symmetrical $S^{d_{x^2-y^2}}_{CDW2} - I - S^{s}_{BCS}$ (a) and $S^{d_{xy}}_{CDW2} - I - S^{s}_{BCS}$ (b) junctions. The parameters of S^{sym}_{CDW2} electrodes are the same as in Fig. 7, and $\delta_{BCS} = 0.1$. See explanations in the text.

Outside the reentrance region of the phase diagram dependences, $i_c(\alpha)$ are monotonic and intuitively clear. Examples of such currents are shown in Fig. 13 for the nonsymmetrical $S^{d_{x^2-y^2}}_{CDW4} - I - S^{s}_{BCS}$ junction. The trend found here correlates with the experimental results [120]. One sees that the increase of the dielectric gap (or, according to our hypothesis concerning the CDW-related pseudogap origin, the temperature of the pseudogap appearance) leads to a rapid decrease of i_c similar to that discussed for the symmetrical case (see Fig. 5).

As for the sample-orientation dependences, nonsymmetrical junctions provide fewer possibilities to our disposal than their symmetrical analogues. Therefore, we shall restrict ourselves only to one representative example. In Fig. 14, the dependences $i_c(\gamma)$ are demonstrated for the junction configuration $S^{d_{x^2-y^2}}_{CDW4} - I - S^{s}_{BCS}$. We see that i_c is suppressed by CDWs for all angles γ, but the general periodic character of dependences characteristic of the junctions concerned does not change.

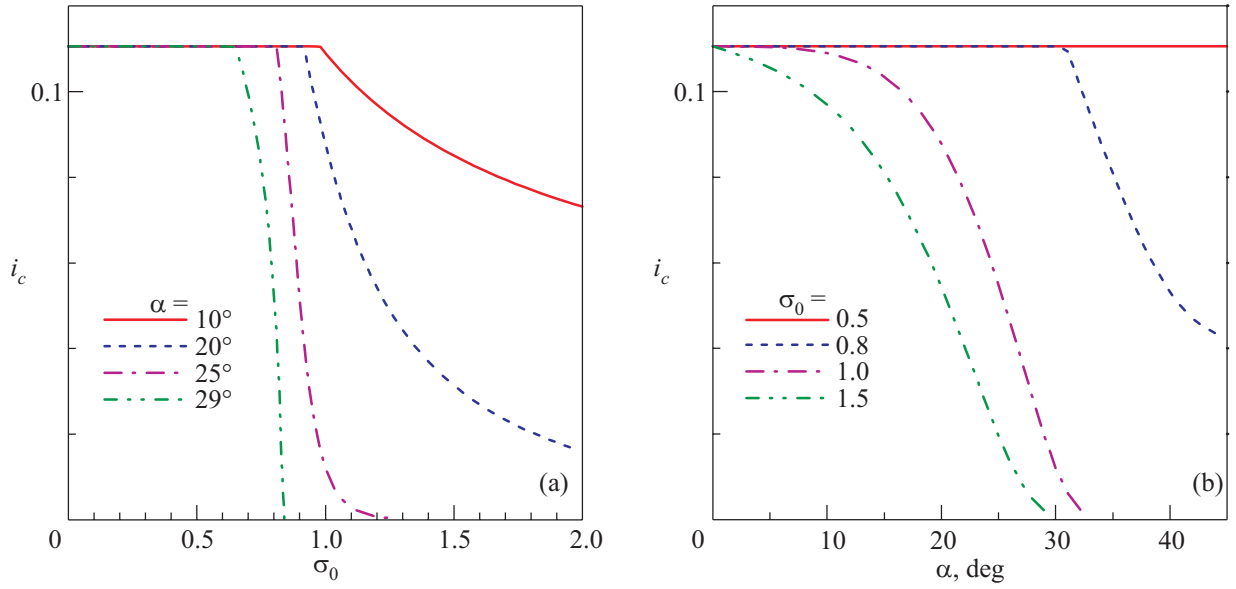

Fig. 13. The same as in Fig. 5, but for the nonsymmetrical $S^{d_{x^2-y^2}}_{CDW4} - I - S^{s}_{BCS}$ junction. The parameters of S^{sym}_{CDW4} electrodes are the same as in Fig. 5, and $\delta_{BCS} = 0.1$.

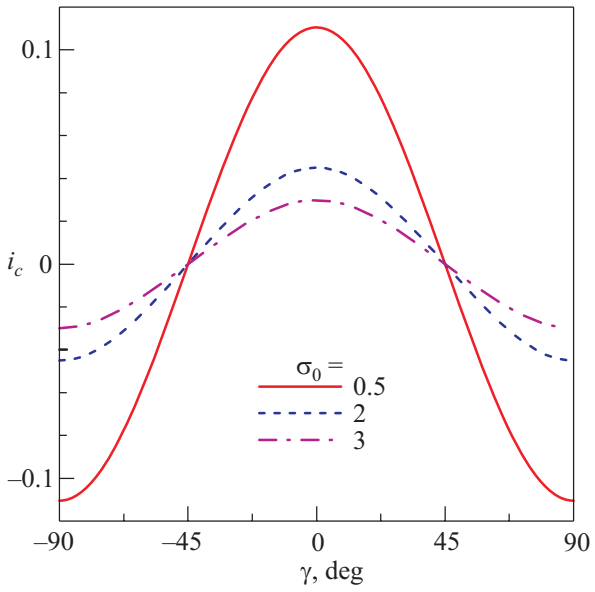

Fig. 14. The same as in Fig. 8(a), but for the nonsymmetrical $S^{d_{x^2-y^2}}_{CDW4} - I - S^{s}_{BCS}$ junction. The parameters of $S^{d_{x^2-y^2}}_{CDW4}$ electrode are the same as in Fig. 8(a), and $\delta_{BCS} = 0.1$.

7. Conclusions

Our results reported here together with the evidence collected earlier [27–32] testify that there are quite a number of superconductors with CDWs. The latter may constitute a true long-range order or cover a finite-range area so that CDW correlations may be regarded sooner as a dynamical fluctuation phenomenon. In both cases, CDWs and superconductivity are antagonists.

For CDW *d*-wave superconductors, the interplay between those two kinds of reconstructed states leads to a number of unusual consequences. In particular, the *T*-reentrance of dielectric order parameter Σ may exist. This behavior of $\Sigma(T)$ could be observed in tunneling spectroscopy or ARPES measurements. On the other hand, the influence of CDWs on superconductivity may result in anomalously large ratios $2\Delta(0)/T_c > 5.5$, which are inherent to high-T_c oxides — especially with underdoped compositions.

Our calculations showed that CDWs can be probed and studied by means of coherent superconducting tunneling. The interplay between CDW manifestations, tunnel directionality, and possible unconventional symmetry of the superconducting order parameter should lead to an involved $i_c(\gamma)$ behavior with two superimposed periodicities in those dependences. Symmetrical junctions (break-junctions, mesas) turn out more suitable in comparison with nonsymmetrical ones (STM) in revealing CDW-related effects.

The results obtained confirm that the dc Josephson current is always suppressed by electron-hole CDW pairing. As concerns the quasiparticle current, the interpretation of experimental results may be much more ambiguous. In particular, the states in the nodal region of FS in *d*-wave superconductors are also engaged into CDW gapping [30–32, 128–130,187] so that the tunnel spectroscopy or/and ARPES feels the overall energy gaps, which are larger than their superconducting constituents.

We demonstrated that the emerging CDWs distort the dependence of the critical Josephson current I_c on the angle γ between a certain crystal axis and the normal **n** to the junction plane, whatever the symmetry of superconducting order parameter is. At the same time, if the *s*-wave contribution to the actual order parameter in a cuprate sample dominates up to the complete disappearance of *d*-wave component, the $I_c(\gamma)$ dependences for junctions involving CDW superconductors are no longer constant in contrast to the CDW-free case. This prediction can be verified for CDW superconductors with a fortiori *s*-wave order parameters (such materials are quite numerous [27–32]).

In this paper, our approach was purely theoretical. We did not discuss unavoidable experimental difficulties if one tries to fabricate Josephson junctions suitable to check the results obtained here. We are fully aware that the emerging problems can be solved on the basis of already accumulated knowledge concerning the nature of grain boundaries in high-T_c oxides [51,188–198]. Note that the required junctions can be created at random in an uncontrollable fashion using the break-junction technique [116]. This method allows the CDW (pseudogap) influence on the tilt-angle dependences to be detected rather easily. In other words, measurements of the Josephson current between an ordinary superconductor and a *d*- or extended *s*-wave one or between two unconventional superconductors (first of all, high-T_c oxides) would be useful for detecting a possible CDW influence on the electron spectrum of electrodes. Similar studies of iron-based superconductors with doping-dependent SDWs would also be of benefit (see, e.g., recent Reviews [147,156,199]), since CDW and SDW superconductors have a number of similar properties [27–29].

Acknowledgments

The authors are grateful to Sergey Borisenko (Leibnitz Institute for Solid State and Materials Research, Dresden) and Alexander Kordyuk (Institute of Metal Physics, Kiev) for useful discussions of cuprate properties and related issues. The work was partially supported by the Project N 8 of the Scientific Cooperation Agreement between Poland and Ukraine in 2012–2014. AIV is grateful to Kasa im. Józefa Mianowskiego, Fundacja na Rzecz Nauki Polskej, and Fundacja Zygmunta Zaleskiego for the financial support of his visits to Warsaw.

1. I.O. Kulik and I.K. Yanson, *Josephson Effect in Superconducting Tunnel Structures*, Israel Program for Scientific Translation, Jerusalem (1972).

2. I.K. Yanson, *Fiz. Nizk. Temp.* **30**, 689 (2004) [*Low Temp. Phys*. **30**, 519 (2004)].
3. Yu.G. Naidyuk and I.K. Yanson, *J. Phys.*: *Condens. Matter* **10**, 8905 (1998).
4. I.K. Yanson and Yu.G. Naidyuk, *Fiz. Nizk. Temp.* **30**, 355 (2004) [*Low Temp. Phys*. **30**, 261 (2004)].
5. Yu.G. Naidyuk and I.K. Yanson, *Point-Contact Spectroscopy*, Springer Verlag, New York (2005).
6. D. Daghero and R.S. Gonnelli, *Supercond. Sci. Technol.* **23**, 043001 (2010).
7. D. Daghero, M. Tortello, G.A. Ummarino, and R.S. Gonnelli, *Rep. Prog. Phys*. **74**, 124509 (2011).
8. P. Monceau, *Adv. Phys*. **61**, 325 (2012).
9. S. Kashiwaya and Y. Tanaka, *Rep. Prog. Phys.* **63**, 1641 (2000).
10. M. Bode, *Rep. Prog. Phys.* **66**, 523 (2003).
11. B. Grandidier, *J. Phys.*: *Condens. Matter* **16**, S161 (2004).
12. Yu.I. Latyshev, P. Monceau, A.P. Orlov, S. Brazovskii, and T. Fournier, *Supercond. Sci. Technol.* **20**, S87 (2007).
13. Ø. Fischer, M. Kugler, I. Maggio-Aprile, and C. Berthod, *Rev. Mod. Phys*. **79**, 353 (2007).
14. A.M. Gabovich, V.A. Drozd, M. Pękała, T. Ekino, and R. Ribeiro, in: *Superconductivity Research Advances*, J.E. Nolan (ed.), Nova Science Publishers, Inc, New York (2007), p. 149.
15. J.F. Zasadzinski, in: *Superconductivity. Novel Superconductors*, K.H. Bennemann and J.B. Ketterson (eds.), Springer Verlag, Berlin (2008), Vol. 2, p. 833.
16. L. Simon, C. Bena, F. Vonau, M. Cranney, and D. Aubel, *J. Phys. D* **44**, 464010 (2011).
17. T. Takasaki, T. Ekino, A.M. Gabovich, A. Sugimoto, S. Yamanaka, and J. Akimitsu, in: *Superconductivity*, V.M. Romanovskii (ed.), Nova Science Publishers, New York (2012), p. 1.
18. R.W. Cahn, *The Coming of Materials Science*, Pergamon Press, Oxford (2001).
19. S. Roth and D. Carroll, *One-Dimensional Metals*, Wiley-VCH, Weinheim (2004).
20. J.M.D. Coey, *Magnetism and Magnetic Materials*, Cambridge University Press, Cambridge (2009).
21. G. Grüner, *Density Waves in Solids*, Addison-Wesley Publishing Company, Reading, Massachusetts (1994).
22. *Physics of Ferroelectrics: A Modern Perspective. Topics in Applied Physics*, K. Rabe, C.H. Ahn, and J-M. Triscone (eds.), Springer Verlag, Berlin (2007), Vol. 105.
23. K. Rossnagel, *J. Phys.*: *Condens. Matter* **23**, 213001 (2011).
24. A.A. Abrikosov, *Fundamentals of the Theory of Metals*, North-Holland, Amsterdam (1988).
25. V.P. Mineev and K.V. Samokhin, *Introduction to Unconventional Superconductivity*, Gordon and Breach, Amsterdam (1999).
26. A.P. Pyatakov and A.K. Zvezdin, *Usp. Fiz. Nauk* **182**, 593 (2012).
27. A.M. Gabovich and A.I. Voitenko, *Fiz. Nizk. Temp.* **26**, 419 (2000) [*Low Temp. Phys.* **26**, 305 (2000)].
28. A.M. Gabovich, A.I. Voitenko, J.F. Annett, and M. Ausloos, *Supercond. Sci. Technol.* **14**, R1 (2001).
29. A.M. Gabovich, A.I. Voitenko, and M. Ausloos, *Phys. Rep.* **367**, 583 (2002).
30. A.M. Gabovich, A.I. Voitenko, T. Ekino, M.S. Li, H. Szymczak, and M. Pękała, *Adv. Condens. Matter Phys*. **2010**, 681070 (2010).
31. T. Ekino, A.M. Gabovich, M.S. Li, M. Pękała, H. Szymczak, and A.I. Voitenko, *Symmetry* **3**, 699 (2011).
32. T. Ekino, A.M. Gabovich, M.S. Li, M. Pękała, H. Szymczak, and A.I. Voitenko, *J. Phys.*: *Condens. Matter* **23**, 385701 (2011).
33. A.M. Gabovich and A.I. Voitenko, *Fiz. Nizk. Temp.* **38**, 414 (2012) [*Low Temp. Phys*. **38**, 326 (2012)].
34. L.R. Testardi, *Rev. Mod. Phys.* **47**, 637 (1975).
35. E.G. Maksimov and O.V. Dolgov, *Usp. Fiz. Nauk* **177**, 983 (2007).
36. E.G. Maksimov, M.L. Kulić, and O.V. Dolgov, *Adv. Condens. Matter Phys*. **2010**, 423725 (2010).
37. Yu.V. Kopaev and A.I. Rusinov, *Phys. Lett. A* **121**, 300 (1987).
38. K. Machida and M. Kato, *Jpn. J. Appl. Phys. Lett*. **26**, L660 (1987).
39. K. Machida and M. Kato, *Phys. Rev. B* **36**, 854 (1987).
40. J. Bardeen, L.N. Cooper, and J.R. Schrieffer, *Phys. Rev.* **108**, 1175 (1957).
41. V.M. Krasnov, A. Yurgens, D. Winkler, P. Delsing, and T. Claeson, *Phys. Rev. Lett.* **84**, 5860 (2000).
42. R.A. Klemm, in: *Nonequilibrium Physics at Short Time Scales. Formation of Correlations*, K. Morawetz (ed.), Springer Verlag, Berlin (2004), p. 381.
43. M. Norman, D. Pines, and C. Kallin, *Adv. Phys.* **54**, 715 (2005).
44. G. Deutscher, *Fiz. Nizk. Temp.* **32**, 740 (2006) [*Low Temp. Phys*. **32**, 566 (2006)].
45. Y. Li, V. Balédent, G. Yu, N. Barišić, K. Hradil, R.A. Mole, Y. Sidis, P. Steffens, X. Zhao, P. Bourges, and M. Greven, *Nature* **468**, 283 (2010).
46. S.I. Vedeneev, *Usp. Fiz. Nauk* **182**, 669 (2012).
47. S.E. Sebastian, N. Harrison, and G.G. Lonzarich, *Rep. Prog. Phys.* **75**, 102501 (2012).
48. T. Yoshida, M. Hashimoto, I.M. Vishik, Z-X. Shen, and A. Fujimori, *J. Phys. Soc. Jpn.* **81**, 011006 (2012).
49. J.F. Annett, N.D. Goldenfeld, and A.J. Leggett, in: *Physical Properties of High Temperature Superconductors V*, D.M. Ginsberg (ed.), World Scientific, River Ridge, NJ (1996), p. 375.
50. R.A. Klemm, *Philos. Mag*. **85**, 801 (2005).
51. J.R. Kirtley, *Rep. Prog. Phys.* **73**, 126501 (2010).
52. G.M. Zhao, *Phys. Scr*. **83**, 038302 (2011).
53. J. Tomaschko, S. Scharinger, V. Leca, J. Nagel, M. Kemmler, T. Selistrovski, D. Koelle, and R. Kleiner, *Phys. Rev. B* **86**, 094509 (2012).
54. E. Morosan, D. Natelson, A.H. Nevidomskyy, and Q. Si, *Adv. Mater*. **24**, 4896 (2012).
55. M. Calandra and F. Mauri, *Phys. Rev. Lett.* **106**, 196406 (2011).
56. S.V. Borisenko, A.A. Kordyuk, A. Yaresko, V.B. Zabolotnyy, D.S. Inosov, R. Schuster, B. Büchner, R. Weber, R.

Follath, L. Patthey, and H. Berger, *Phys. Rev. Lett.* **100**, 196402 (2008).
57. D.S. Inosov, V.B. Zabolotnyy, D.V. Evtushinsky, A.A. Kordyuk, B. Büchner, R. Follath, H. Berger, and S.V. Borisenko, *New J. Phys.* **10**, 125027 (2008).
58. S.V. Borisenko, A.A. Kordyuk, V.B. Zabolotnyy, D.S. Inosov, D. Evtushinsky, B. Büchner, A.N. Yaresko, A. Varykhalov, R. Follath, W. Eberhardt, L. Patthey, and H. Berger, *Phys. Rev. Lett.* **102**, 166402 (2009).
59. D.S. Inosov, D.V. Evtushinsky, V.B. Zabolotnyy, A.A. Kordyuk, B. Büchner, R. Follath, H. Berger, and S.V. Borisenko, *Phys. Rev. B* **79**, 125112 (2009).
60. Ph. Leininger, D. Chernyshov, A. Bosak, H. Berger, and D.S. Inosov, *Phys. Rev. B* **83**, 233101 (2011).
61. F. Weber, S. Rosenkranz, J-P. Castellan, R. Osborn, R. Hott, R. Heid, K-P. Bohnen, T. Egami, A.H. Said, and D. Reznik, *Phys. Rev. Lett.* **107**, 107403 (2011).
62. A.D. Hillier, P. Manue, D.T. Adroja, J.W. Taylor, A.K. Azad, and J.T.S. Irvine, *Phys. Rev. B* **81**, 092507 (2010).
63. F. Marsiglio and J.P. Carbotte, in: *Superconductivity. Conventional and Unconventional Superconductors*, K.H. Bennemann and J.B. Ketterson (eds.), Springer Verlag, Berlin (2008), Vol. 1, p. 73.
64. S.C. Lo and K.W. Wong, *Nuovo Cimento B* **10**, 383 (1972).
65. A.M. Gabovich, E.A. Pashitskii, and A.S. Shpigel, *Fiz. Tverd. Tela* **21**, 463 (1979).
66. M. Iavarone, R. Di Capua, X. Zhang, M. Golalikhani, S.A. Moore, and G. Karapetrov, *Phys. Rev. B* **85**, 155103 (2012).
67. J. van Wezel, P. Nahai-Williamson, and S.S. Saxena, *Phys. Rev. B* **81**, 165109 (2010).
68. C. Monney, E.F. Schwier, M.G. Garnier, N. Mariotti, C. Didiot, H. Beck, P. Aebi, C. Battaglia, H. Berger, and A.N. Titov, *Phys. Rev. B* **81**, 155104 (2010).
69. M.M. May, C. Brabetz, C. Janowitz, and R. Manzke, *Phys. Rev. Lett.* **107**, 176405 (2011).
70. E. Morosan, K.E. Wagner, L.L. Zhao, Y. Hor, A.J. Williams, J. Tao, Y. Zhu, and R.J. Cava, *Phys. Rev. B* **81**, 094524 (2010).
71. A. Damascelli, Z. Hussain, and Z-X. Shen, *Rev. Mod. Phys.* **75**, 473 (2003).
72. R.S. Markiewicz, *J. Phys. Chem. Solidi* **58**, 1179 (1997).
73. A.M. Gabovich, *Fiz. Tverd. Tela* **22**, 3231 (1980).
74. P. Xu, J.O. Piatek, P-H. Lin, B. Sipos, H. Berger, L. Forró, H.M. Rønnow, and M. Grioni, *Phys. Rev. B* **81**, 172503 (2010).
75. J. Zittartz, *Phys. Rev.* **164**, 575 (1967).
76. H.G. Schuster, *Solid State Commun.* **14**, 127 (1974).
77. L.J. Li, W.J. Lu, X.D. Zhu, L.S. Ling, Z. Qu, and Y.P. Sun, *Europhys. Lett.* **97**, 67005 (2012).
78. J.A. Wilson, F.J. Di Salvo, and S. Mahajan, *Adv. Phys.* **24**, 117 (1975).
79. I. Guillamón, H. Suderow, J.G. Rodrigo, S. Vieira, P. Rodière, L. Cario, E. Navarro-Moratalla, C. Martí-Gastaldo, and E. Coronado, *New J. Phys.* **13**, 103020 (2011).
80. J. Ishioka, Y.H. Liu, K. Shimatake, T. Kurosawa, K. Ichimura, Y. Toda, M. Oda, and S. Tanda, *Phys. Rev. Lett.* **105**, 176401 (2010).
81. D.J. Rahn, S. Hellmann, M. Kalläne, C. Sohrt, T.K. Kim, L. Kipp, and K. Rossnagel, *Phys. Rev. B* **86**, 224532 (2012).
82. D.E. Moncton, J.D. Axe, and F.J. DiSalvo, *Phys. Rev. B* **16**, 801 (1977).
83. J.J. Yang, Y.J. Choi, Y.S. Oh, A. Hogan, Y. Horibe, K. Kim, B.I. Min, and S-W. Cheong, *Phys. Rev. Lett.* **108**, 116402 (2012).
84. D.I. Khomskii and T. Mizokawa, *Phys. Rev. Lett.* **94**, 156402 (2005).
85. G. Bilbro and W.L. McMillan, *Phys. Rev. B* **14**, 1887 (1976).
86. A.M. Gabovich, D.P. Moiseev, and A.S. Shpigel, *J. Phys. C* **15**, L569 (1982).
87. K. Yamaya, S. Takayanagi, and S. Tanda, *Phys. Rev. B* **85**, 184513 (2012).
88. X. Zhu, H. Lei, and C. Petrovic, *Phys. Rev. Lett.* **106**, 246404 (2011).
89. C.S. Yadav and P.L. Paulose, *J. Phys.*: *Condens. Matter* **24**, 235702 (2012).
90. A.M. Gabovich, M.S. Li, H. Szymczak, and A.I. Voitenko, *J. Phys.*: *Condens. Matter* **15**, 2745 (2003).
91. H. Lei, X. Zhu, and C. Petrovic, *Europhys. Lett.* **95**, 17011 (2011).
92. K.C. Rahnejat, C.A. Howard, N.E. Shuttleworth, S.R. Schofield, K. Iwaya, C.F. Hirjibehedin, Ch. Renner, G. Aeppli, and M. Ellerby, *Nat. Commun.* **2**, 558 (2011).
93. T.E. Weller, M. Ellerby, S.S. Saxena, R.P. Smith, and N.T. Skipper, *Nature Phys.* **1**, 39 (2005).
94. N.S. Sangeetha, A. Thamizhavel, C.V. Tomy, S. Basu, A.M. Awasthi, S. Ramakrishnan, and D. Pal, *Phys. Rev. B* **86**, 024524 (2012).
95. M.H. Lee, C.H. Chen, M-W. Chu, C.S. Lue, and Y.K. Kuo, *Phys. Rev. B* **83**, 155121 (2011).
96. M.C. Boyer, W.D. Wise, K. Chatterjee, M. Yi, T. Kondo, T. Takeuchi, H. Ikuta, and E.W. Hudson, *Nature Phys.* **3**, 802 (2007).
97. M.A. Krivoglaz, *Usp. Fiz. Nauk* **111**, 617 (1973).
98. E.L. Nagaev, *Usp. Fiz. Nauk* **165**, 529 (1995) [*Phys. Usp.* **38**, 497 (1995)].
99. J.M. Tranquada, in: *Neutron Scattering in Layered Copper-Oxide Superconductors*, A. Furrer (ed.), Kluwer Academic, Dordrecht (1998), p. 225.
100. E. Dagotto, T. Hotta, and A. Moreo, *Phys. Rep.* **344**, 1 (2001).
101. M.Yu. Kagan and K.I. Kugel, *Usp. Fiz. Nauk* **171**, 577 (2001).
102. E. Dagotto, S. Yunoki, C. Şen, G. Alvarez, and A. Moreo, *J. Phys.*: *Condens. Matter* **20**, 434224 (2008).
103. D.S. Inosov, A. Leineweber, X. Yang, J.T. Park, N.B. Christensen, R. Dinnebier, G.L. Sun, Ch. Niedermayer, D. Haug, P.W. Stephens, J. Stahn, O. Khvostikova, C.T. Lin, O.K. Andersen, B. Keimer, and V. Hinkov, *Phys. Rev. B* **79**, 224503 (2009).
104. P.M. Grant, *Nature* **476**, 37 (2011).
105. G. Seibold, M. Grilli, and J. Lorenzana, *Physica C* **481**, 132 (2012).

106. J.R. Neilson, A. Llobet, A.V. Stier, L. Wu, J. Wen, J. Tao, Y. Zhu, Z.B. Tesanovic, N.P. Armitage, and T.M. McQueen, *Phys. Rev. B* **86**, 054512 (2012).
107. T. Koyama, Y. Ozaki, K. Ueda, T. Mito, T. Kohara, T. Waki, Y. Tabata, C. Michioka, K. Yoshimura, M-T. Suzuki, and H. Nakamura, *Phys. Rev. B* **84**, 212501 (2011).
108. Y-L. Sun, H. Jiang, H-F. Zhai, J-K. Bao, W-H. Jiao, Q. Tao, C-Y. Shen, Y-W. Zeng, Z-A. Xu, and G-H. Cao, *J. Am. Chem. Soc.* **134**, 12893 (2012).
109. K. Fujita, A.R. Schmidt, E-A. Kim, M.J. Lawler, D.H. Lee, J.C. Davis, H. Eisaki, and S-i. Uchida, *J. Phys. Soc. Jpn.* **81**, 011005 (2012).
110. S-i. Uchida, *Jpn. J. Appl. Phys.* **51**, 010002 (2012).
111. T. Tohyama, *Jpn. J. Appl. Phys.* **51**, 010004 (2012).
112. M. Hücker, *Physica C* **481**, 3 (2012).
113. D. Reznik, *Physica C* **481**, 75 (2012).
114. T. Valla, *Physica C* **481**, 66 (2012).
115. Y. Toda, T. Mertelj, P. Kusar, T.K.M. Oda, M. Ido, and D. Mihailovic, *Phys. Rev. B* **84**, 174516 (2011).
116. T. Ekino, Y. Sezaki, and H. Fujii, *Phys. Rev. B* **60**, 6916 (1999).
117. Y.H. Liu, Y. Toda, K. Shimatake, N. Momono, M. Oda, and M. Ido, *Phys. Rev. Lett.* **101**, 137003 (2008).
118. V.M. Krasnov, A.E. Kovalev, A. Yurgens, and D. Winkler, *Phys. Rev. Lett.* **86**, 2657 (2001).
119. T. Ekino, A.M. Gabovich, M.S. Li, M. Pękała, H. Szymczak, and A.I. Voitenko, *Phys. Rev. B* **76**, 180503 (2007).
120. M. Suzuki, T. Hamatani, K. Anagawa, and T. Watanabe, *Phys. Rev. B* **85**, 214529 (2012).
121. J.W. Alldredge, K. Fujita, H. Eisaki, S. Uchida, and K. McElroy, *Phys. Rev. B* **85**, 174501 (2012).
122. A.R. Schmidt, K. Fujita, E-A. Kim, M.J. Lawler, H. Eisaki, S. Uchida, D-H. Lee, and J.C. Davis, *New J. Phys.* **13**, 065014 (2011).
123. Y. Okada, Y. Kuzuya, T. Kawaguchi, and H. Ikuta, *Phys. Rev. B* **81**, 214520 (2010).
124. T. Hu, H. Xiao, P. Gyawali, H.H. Wen, and C.C. Almasan, *Phys. Rev. B* **85**, 134516 (2012).
125. A. Piriou, N. Jenkins, C. Berthod, I. Maggio-Aprile, and Ø. Fischer, *Nat. Commun*. **2**, 221 (2011).
126. J. Nieminen, I. Suominen, T. Das, R.S. Markiewicz, and A. Bansil, *Phys. Rev. B* **85**, 214504 (2012).
127. M. Hashimoto, R-H. He, I.M. Vishik, F. Schmitt, R.G. Moore, D.H. Lu, Y. Yoshida, H. Eisaki, Z. Hussain, T.P. Devereaux, and Z-X. Shen, *Phys. Rev. B* **86**, 094504 (2012).
128. A.M. Gabovich and A.I. Voitenko, *Phys. Rev. B* **80**, 224501 (2009).
129. A.I. Voitenko and A.M. Gabovich, *Fiz. Nizk. Temp.* **36**, 1300 (2010) [*Low Temp. Phys*. **36**, 1049 (2010)].
130. A.I. Voitenko and A.M. Gabovich, *Fiz. Tverd. Tela* **52**, 20 (2010).
131. Y. Kohsaka, T. Hanaguri, M. Azuma, M. Takano, J.C. Davis, and H. Takagi, *Nature Phys*. **8**, 534 (2012).
132. A.M. Gabovich and A.I. Voitenko, *Phys. Rev. B* **75**, 064516 (2007).
133. T. Ekino, A.M. Gabovich, and A.I. Voitenko, *Fiz. Nizk. Temp.* **34**, 515 (2008) [*Low Temp. Phys*. **34**, 409 (2008)].
134. N. Poccia, A. Ricci, G. Campi, M. Fratini, A. Puri, D. Di Gioacchino, A. Marcelli, M. Reynolds, M. Burghammer, N.L. Saini, G. Aeppli, and A. Bianconi, *Proc. Nat. Acad. Sci. USA* **109**, 15685 (2012).
135. M.V. Sadovskii, *Usp. Fiz. Nauk* **171**, 539 (2001).
136. E.A. Nowadnick, B. Moritz, and T.P. Devereaux, *Phys. Rev. B* **86**, 134509 (2012).
137. R. Collongues, *La Non-Stoechiometrie*, Masson, Paris (1971).
138. B. Raveau, *Phys. Today* **45**, 53 (October 1992).
139. N. Poccia, G. Campi, M. Fratini, A. Ricci, N.L. Saini, and A. Bianconi, *Phys. Rev. B* **84**, 100504 (2011).
140. H.L. Edwards, D.J. Derro, A.L. Barr, J.T. Markert, and A.L. de Lozanne, *Phys. Rev. Lett.* **75**, 1387 (1995).
141. V.B. Zabolotnyy, A.A. Kordyuk, D. Evtushinsky, V.N. Strocov, L. Patthey, T. Schmitt, D. Haug, C.T. Lin, V. Hinkov, B. Keimer, B. Büchner, and S.V. Borisenko, *Phys. Rev. B* **85**, 064507 (2012).
142. G. Ghiringhelli, M. Le Tacon, M.M.S. Blanco-Canosa, C. Mazzoli, N.B. Brookes, G.M. De Luca, A. Frano, D.G. Hawthorn, F. He, T. Loew, M.M. Sala, D.C. Peets, M. Salluzzo, E. Schierle, R. Sutarto, G.A. Sawatzky, E. Weschke, B. Keimer, and L. Braicovich, *Science* **337**, 821 (2012).
143. S.J. Moon, A.A. Schafgans, S. Kasahara, T. Shibauchi, T. Terashima, Y. Matsuda, M.A. Tanatar, R. Prozorov, A. Thaler, P.C. Canfield, A.S. Sefat, D. Mandrus, and D.N. Basov, *Phys. Rev. Lett.* **109**, 027006 (2012).
144. Y-M. Xu, P. Richard, K. Nakayama, T. Kawahara, Y. Sekiba, T. Qian, M. Neupane, S. Souma, T. Sato, T. Takahashi, H-Q. Luo, H-H. Wen, G-F. Chen, N-L. Wang, Z. Wang, Z. Fang, X. Dai, and H. Ding, *Nat. Commun*. **2**, 394 (2011).
145. K. Machida, *J. Phys. Soc. Jpn.* **50**, 2195 (1981).
146. P. Cai, C. Ye, W. Ruan, X. Zhou, A. Wang, M. Zhang, X. Chen, and Y. Wang, *Phys. Rev. B* **85**, 094512 (2012).
147. A. Chubukov, *Annu. Rev. Condens. Matter Phys.* **3**, 57 (2012).
148. W. Li, S. Dong, C. Fang, and J. Hu, *Phys. Rev. B* **85**, 100407 (2012).
149. H. Won and K. Maki, *Phys. Rev. B* **49**, 1397 (1994).
150. A.A. Kordyuk, V.B. Zabolotnyy, D.V. Evtushinsky, D.S. Inosov, T.K. Kim, B. Büchner, and S.V. Borisenko, *Eur. Phys. J. Special Topics* **188**, 153 (2010).
151. T.M. Rice, K-Y. Yang, and F.C. Zhang, *Rep. Prog. Phys.* **75**, 016502 (2012).
152. N. Harrison and S.E. Sebastian, *New J. Phys.* **14**, 095023 (2012).
153. A.I. Voitenko and A.M. Gabovich, *Fiz. Tverd. Tela* **49**, 1356 (2007).
154. D.S. Inosov, J.T. Park, A. Charnukha, Y. Li, A.V. Boris, B. Keimer, and V. Hinkov, *Phys. Rev. B* **83**, 214520 (2011).
155. P.B. Allen and B. Mitrović, *Solid State Phys*. **37**, 1 (1982).
156. G.R. Stewart, *Rev. Mod. Phys.* **83**, 1589 (2011).

157. A.E. Gorbonosov and I.O. Kulik, *Fiz. Met. Metalloved*. **23**, 803 (1967).
158. M. Ledvij and R.A. Klemm, *Phys. Rev. B* **51**, 3269 (1995).
159. P. Pairor and M.F. Smith, *J. Phys.*: *Condens. Matter* **15**, 4457 (2003).
160. A.M. Gabovich, D.P. Moiseev, A.S. Shpigel, and A.I. Voitenko, *Phys. Status Solidi B* **161**, 293 (1990).
161. Yu.S. Barash, A.V. Galaktionov, and A.D. Zaikin, *Phys. Rev. B* **52**, 665 (1995).
162. Yu.S. Barash, H. Burkhardt, and D. Rainer, *Phys. Rev. Lett.* **77**, 4070 (1996).
163. Yu.S. Barash, A.V. Galaktionov, and A.D. Zaikin, *Phys. Rev. Lett.* **75**, 1676 (1995).
164. A. Sharoni, G. Leibovitch, A. Kohen, R. Beck, G. Deutscher, G. Koren, and O. Millo, *Europhys. Lett.* **62**, 883 (2003).
165. C. Bruder, A. van Otterlo, and G.T. Zimanyi, *Phys. Rev. B* **51**, 12904 (1995).
166. V. Ambegaokar and A. Baratoff, *Phys. Rev. Lett.* **10**, 486 (1963).
167. V. Ambegaokar and A. Baratoff, *Phys. Rev. Lett.* **11**, 104 (1963).
168. M. Sigrist and T.M. Rice, *J. Phys. Soc. Jpn.* **61**, 4283 (1992).
169. G.E. Blonder, M. Tinkham, and T.M. Klapwijk, *Phys. Rev. B* **25**, 4515 (1982).
170. A.F. Andreev, *Zh. Éksp. Teor. Fiz*. **46**, 1823 (1964) [*Sov. Phys*. *JETP* **19**, 1228 (1964)].
171. D. Saint-James, *J. Phys. (Paris)* **25**, 899 (1964).
172. G. Deutscher, *Rev. Mod. Phys.* **77**, 109 (2005).
173. A.I. Voitenko, A.M. Gabovich, D.P. Moiseev, V.M. Postnikov, and A.S. Shpigel, *Fiz. Nizk. Temp.* **16**, 283 (1990) [*Sov. Low Temp. Phys*. **16**, 154 (1990)].
174. T. Ekino, S. Hashimoto, T. Takasaki, and H. Fujii, *Phys. Rev. B* **64**, 092510 (2001).
175. A.A. Kordyuk, S.V. Borisenko, M.S. Golden, S. Legner, K.A. Nenkov, M. Knupfer, J. Fink, H. Berger, L. Forró, and R. Follath, *Phys. Rev. B* **66**, 014502 (2002).
176. W.S. Lee, I.M. Vishik, K. Tanaka, D.H. Lu, T. Sasagawa, N. Nagaosa, T.P. Devereaux, Z. Hussain, and Z-X. Shen, *Nature* **450**, 81 (2007).
177. T. Ekino, A.M. Gabovich, M.S. Li, M. Pękała, H. Szymczak, and A.I. Voitenko, *J. Phys.*: *Condens. Matter* **20**, 425218 (2008).
178. A.A. Kordyuk, S.V. Borisenko, V.B. Zabolotnyy, R. Schuster, D.S. Inosov, D.V. Evtushinsky, A.I. Plyushchay, R. Follath, A. Varykhalov, L. Patthey, and H. Berger, *Phys. Rev. B* **79**, 020504 (2009).
179. T. Kurosawa, T. Yoneyama, Y. Takano, M. Hagiwara, R. Inoue, N. Hagiwara, K. Kurusu, K. Takeyama, N. Momono, M. Oda, and M. Ido, *Phys. Rev. B* **81**, 094519 (2010).
180. I.M. Vishik, W.S. Lee, R-H. He, M. Hashimoto, Z. Hussain, T.P. Devereaux, and Z-X. Shen, *New J. Phys.* **12**, 105008 (2010).
181. A.A. Kordyuk, V.B. Zabolotnyy, D.V. Evtushinsky, B. Büchner, and S.V. Borisenko, *J. Electron Spectrosc. Relat. Phenom*. **181**, 44 (2010).
182. T. Kondo, Y. Hamaya, A.D. Palczewski, T. Takeuchi, J.S. Wen, Z.J. Xu, G. Gu, J. Schmalian, and A. Kaminski, *Nature Phys*. **7**, 21 (2011).
183. R-H. He, M. Hashimoto, H. Karapetyan, J.D. Koralek, J.P. Hinton, J.P. Testaud, V. Nathan, Y. Yoshida, H. Yao, K. Tanaka, W. Meevasana, R.G. Moore, D.H. Lu, S-K. Mo, M. Ishikado, H. Eisaki, Z. Hussain, T.P. Devereaux, S.A. Kivelson, J. Orenstein, A. Kapitulnik, and Z-X. Shen, *Science* **331**, 1579 (2011).
184. J-Q. Meng, M. Brunner, K-H. Kim, H-G. Lee, S-I. Lee, J.S. Wen, Z.J. Xu, G.D. Gu, and G-H. Gweon, *Phys. Rev. B* **84**, 060513 (2011).
185. H-B. Yang, J.D. Rameau, Z-H. Pan, G.D. Gu, P.D. Johnson, H. Claus, D.G. Hinks, and T.E. Kidd, *Phys. Rev. Lett.* **107**, 047003 (2011).
186. M. Suzuki, R. Takemura, K. Hamada, M. Ohmaki, and T. Watanabe, *Jpn. J. Appl. Phys.* **51**, 010112 (2012).
187. G. Koren and N. Levy, *Europhys. Lett.* **59**, 121 (2002).
188. S.E. Babcock and J.L. Vargas, *Annu. Rev. Mater. Sci*. **25**, 193 (1995).
189. H. Hilgenkamp, J. Mannhart, and B. Mayer, *Phys. Rev. B* **53**, 14586 (1996).
190. J. Mannhart and P. Chaudhari, *Phys. Today* **54**, 48 (November 2001).
191. C.W. Schneider, H. Bielefeldt, B. Goetz, G. Hammerl, A. Schmehl, R.R. Schulz, H. Hilgenkamp, and J. Mannhart, *Curr. Appl. Phys*. **1**, 349 (2001).
192. W.K. Neils, D.J. Van Harlingen, S. Oh, J.N. Eckstein, G. Hammerl, J. Mannhart, A. Schmehl, C.W. Schneider, and R.R. Schulz, *Physica C* **368**, 261 (2002).
193. H. Hilgenkamp and J. Mannhart, *Rev. Mod. Phys.* **74**, 485 (2002).
194. A.A. Golubov, M.Yu. Kupriyanov, and E. Il'ichev, *Rev. Mod. Phys.* **76**, 411 (2004).
195. F. Tafuri, J.R. Kirtley, F. Lombardi, P.G. Medaglia, P. Orgiani, and G. Balestrino, *Fiz. Nizk. Temp.* **30**, 785 (2004) [*Low Temp. Phys*. **30**, 591 (2004)].
196. F. Tafuri and J.R. Kirtley, *Rep. Prog. Phys.* **68**, 2573 (2005).
197. A.A. Aligia, A.P. Kampf, and J. Mannhart, *Phys. Rev. Lett.* **94**, 247004 (2005).
198. S. Graser, P.J. Hirschfeld, T. Kopp, R. Gutser, B.M. Andersen, and J. Mannhart, *Nature Phys*. **6**, 609 (2010).
199. A.A. Kordyuk, *Fiz. Nizk. Temp.* **38**, 1119 (2012) [*Low Temp. Phys*. **38**, 888 (2012)].